ANALYSIS, SIMULATION, AND CONTROL OF BLINDFOLDED WALKING

THESIS

Presented in Partial Fulfilment of the Requirements for Graduation with Honors Research Distinction from Department of Mechanical and Aerospace Engineering at

The Ohio State University

By

Kaiwen Yang

Undergraduate Program in Mechanical Engineering and Mathematics

The Ohio State University

2017

Thesis Committee:

Manoj Srinivasan, Advisor

Prasad Mokashi, Committee Member

Abstract

People can walk fairly straight with their vision because vision provides the sensory feedback needed to control our movement direction robustly. However, without vision, for instance, when people are blindfolded, they cannot in general walk straight even if they think they can. No quantitatively accurate theory has been able to explain why individuals perform blindfolded walking so differently and explain the heading angle deviation in the blindfolded walking and what causes people not to be able to walk with a solid heading angle without using their eyes. In this research, we use human subject experiments to explore how physical asymmetries in blindfolded walking (specifically, introducing a weight to only one side of the angle, adding a knee brace, sound frequency) affect being able to walk in a straight line and how much the resulting deviation is caused by a certain physical asymmetry. We found that the asymmetric knee brace and the asymmetric sound input affected the trajectories of blindfolded walking, causing them to turn in a systematic direction, although there was considerable trial-to-trial variability in turning behavior. In addition to these experiments, we obtain a probabilistic model to simulate blindfolded walking trials based on data from normal walking data (without blindfolds). This simple probabilistic model simulates curved trajectories as observed in blindfolded walking. Normal people will not do blindfolded walking in daily life, but such blindfolded walking simulates the experience of blind people or people with limited vision. The unpredictability of the blindfolded walking can lead to a severe safety hazard. It would be useful to develop a portable robotic or sensory augmentation device to guide those people to

walk straight. Our goal is to build a device using GPS and vibration feedback to correct blindfolded walking trajectories, for which we present ongoing work on device development.

Dedication

Dedicated to The Ohio State University

Acknowledgements

I am indebted to Dr. Manoj Srinivasan for his mentorship on biomechanics and robotics.

Also, I thank all subjects in this research for their collaboration and patience, and I thank college of engineering for awarding me the research fund.

Table of Contents

List of Figures/ Tables

Chapter 1: Introduction

1.1 Background and related work

Humans can walk straight with vision because eyes serve as a robust target sensor and a compass for determining direction. Without vision, human walk without a clear sense of direction, and walking straight becomes a difficult task.

Scholars from many disciplines like neuroscience and biomechanics researched on how human's walk without vision or walk on a terrain without visual target, or similar topics, for example, undirected walking or walking without a compass. In the paper "Walking Straight into Circles", Souman et al [1] had subjects walk on unfamiliar terrain without external directional reference (large forest area and Sahara desert), and they found that subject cannot walk straight for a long time and perform even worse if they cannot see the sun or other identifying markers like clouds [1].

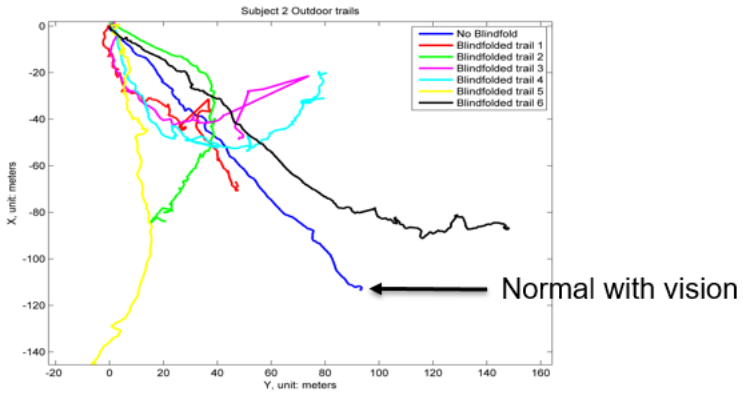

Figure 1: Short distance blindfolded walking trials. [2]

Sijie Yu, an undergraduate researcher in Ohio State Movement Lab, analyzed how people walk without vision for a short distance. He also found great complexity and unpredictability in this

kind of abnormal walking. Especially, the experimental veering behaviors are particularly hard to be predicted using a simple mathematical model [2]. As shown in Figure 1, the blue line is subject walking with vision while lines with other colors are blindfolded walking trials. Subject's walking trajectories did not show a systematic veering direction. Souman et al explained these veering behaviors by "Functional Asymmetries". Bestaven et al [3] also pointed out that people tend to walk around circle without vision may due to postural asymmetry. Similarly, but from a different perspective, Kallie CS et al [4] address the variable error in individual steps as the most important factor to the veering behavior in the paper "Variability in stepping direction explains the veering behavior of blind walkers."

Cheung et al. [5] in the paper pointed out that the extreme consequences of navigating without a compass have not been properly quantified or appreciated. Therefore, they created a mathematical model by regulating the distribution of forwarding distance and heading angle within a rather simple iterative process to see the deviation and variety in the possible trajectories. They did quantitative analysis based on this model and evaluated the expectation and deviation of trajectories from a different perspective. However, this mathematical model did not take the "functional asymmetry" and "postural asymmetry" into account by only considering the heading angle and heading distance. Further, their model of movement variability was not based on detailed human walking data. Animal movement (including human walking) is more complicated than this model described and consisted of other essential factors that must be integrated into a solid mathematical model.

Other than asymmetric nature of our body, there are even more factors contributing to the complexity of the blindfolded walking. The other factor is the stochastic nature of muscle

activation. When we walk, many muscles are engaged, and our muscles work in a stochastic way, meaning that the exert force cannot be precisely controlled by our brain even if we do the same operation again and again [6]. Another factor is that we walk on terrain that is not perfectly flat. All these random factors make the dynamics of the blindfolded walking more complex.

On the other hand, studying blindfolded walking is important. It gives us a big picture of the functional feature of the human body as a walking mechanism. By inspecting a subject's blindfolded walking behavior, we may be able to reveal the how vision is used to correct walking direction errors as well as provide information about individual's unique body and movement asymmetries. This kind of information cannot be simply observed from people's normal walking with vision. Further, by studying blindfolded walking, it helps us get an idea of how blind people walk. While there are differences between blind people walking and blindfolded walking, Kallie et al [4] noted that: "No significant differences in the shapes of veering trajectories were found between blind and blindfolded participants."

1.2 Research objectives

In the research presented in this thesis, blindfolded experiments and blindfolded walking simulation were performed. Since "functional asymmetry" and "postural asymmetry" have been recognized by multiple scholars as a possible reason for why people cannot walk straight without vision, we externally created asymmetric factors into blindfolded walking and see if these asymmetric factors can lead to a uniform veering behavior. Three asymmetric constraints were introduced: single-sided ankle weight, single-sided knee brace, and asymmetric sound

instruction. During the experiment, one of three constraints was applied as the subject was conducting blindfolded walking and GPS logger recorded their walking trajectories.

Secondly, we developed a mathematical model to predict subject's blindfolded walking behavior from their normal walking data. This mathematical model takes walking asymmetry, walking pattern and random noise of muscle into consideration and gives a reasonable prediction of subjects' possible blindfolded walking behavior.

Finally, we developed an algorithm and implemented on a sensory augmentation device to help blindfolded people or even blind people to walk straight. Moreover, more sophisticated algorithm was provided to help navigation in a more complex situation in other navigation devices.

1.3 Overview of the thesis

In Chapter 2, the methods and results of the asymmetric blindfolded walking experiment is introduced and explained in detail. Chapter 3 develops a blindfolded mathematical model from normal walking data. Simulation results from the model are also shown along with some other interesting observation that can be verified via future experiments. In chapter 4, we briefly describe ongoing work on sensory augmentation device algorithm and the design of such hardware. Chapter 5 gives a conclusion and some suggestions for future work.

Chapter 2: Blindfolded Walking Experiment with Physical Asymmetric Constraints

2.1 Introduction

Normal blindfolded walking is quite complicated and quite unpredictable because human body, a bipedal mechanism, has too many degrees of freedom and the bipedal walking process involves multiple muscle actuation and complex neural stability control [7]. Prior studies found that subjects differ from one another when conducting blindfolded walking and trajectories generated from multiple trials can lead to a converging observation on subjects' individual blindfolded bias [2]. However, these individual walking habits do not tell us what factors will affect general human walking when they don't have vision.

To study what factors may affect blindfolded walking trajectories, we introduce reasonable asymmetric factors into blindfolded walking trials to see how subject react to the asymmetry and what trends show uniformly among the subjects.

Three kinds of asymmetric constraints were introduced into the blindfolded walking trials: single-sided ankle weight, single-sided knee brace and asymmetric metronome audio feedback on each ear (see Figure 2). These three asymmetric constraints were added towards three critical joints and sensors of walking that can potentially change the normal walking mechanism. By adding an ankle weight on one side of the ankle, the weight of one leg increases while the other leg's weight remains unchanged, causing the increase of metabolic cost to raise the weighted leg to the same height as well as the cost to maintain walking symmetry. By adding a knee brace on one leg, we change the impedance of relative rotation between femur

and tibia, affecting not only the actuation force but also the stride length when walking. Finally, by giving asymmetric stepping instruction through metronome audio, the swing time of two legs will be different which may result in different stride length between two legs as well as the trajectory since the trajectory is just the set of iterative foot stepping points.

2.2 General experiment setup

The experimental protocol was approved by the Ohio State University IRB and all subjects provided informed consent. Experiments were conducted at Fred Beekman Park, The Ohio State University, 2200 Carmack Rd on the flat baseball court. Subjects were blindfolded by a headband in front of their eyes and constrained by either an ankle weight, knee brace or a headphone with asymmetric sound. The subjects are instructed to walk forward as naturally as possible. Subjects wear a GPS logger operating at 10Hz at pelvis point with an antenna fixed on their head.

Figure 2: Experiment instrumentation

Each trial lasted about 60 seconds, and each subject did at least nine trials starting and ending with two plain blindfolded trials. Trial sequence including different constraints was randomized

and subjects take a reasonable amount of time to break between trials so that the result of each trial was uncorrelated and independent. Table 1 shows a sample trial plan.

Table 1: A sample trial plan

Trial No.	Vision	Constrain Part	Left/Right	Intensity
1	Yes	N/A	N/A	N/A
2	No	Ankle	Left	M
3	No	knee	Left	I1
4	No	Knee	Right	I2
5	No	ANKLE	Right	2M
6	No	Knee	Left	I2
7	No	ANKLE	Left	2M
8	No	Knee	Right	I1
9	No	ANKLE	Right	M

There were ten healthy subjects in total, and they were divided into two groups. One group of 6 subjects did ankle and knee constraint experiments while the other group of four subjects did sound experiments. The first group consists of two female subjects and four male subjects with an average age of 26 years, average height 1.76 m, and average mass 80 kg. The second group consists of two female subjects and two male subjects with an average age of 24 years, average height 1.68 m, and average mass 67 kg. Their walking performance was video recorded for the duration of the trials.

2.3 Data Processing

Raw GPS data provides the subject position in terms of latitude and longitude, which form a 'geodetic' coordinate system. To study the trajectory of subject's walking, some assumptions are made to make data processing easier. Firstly, the earth is assumed to be a sphere when converting geodetic coordinate to ECEF (Earth Centered Earth Fixed) coordinate even though the earth is better approximated as an ellipsoid. Let us define ϕ, λ and h to be latitude, longitude and altitude. Define $N(\phi)$ as $\frac{a^2}{\sqrt{a^2 cos\phi^2 + b^2 sin\phi^2}}$, where a and b are principal axes of the earth's axisymmetric ellipsoidal shape. Then ECEF coordinate can be converted using the following formulas [8]:

$$x = (N(\phi) + h)cos\phi cos\lambda$$

$$y = (N(\phi) + h)cos\phi sin\lambda$$

$$z = \left(\frac{b^2}{a^2} N(\phi) + h\right) sin\phi$$

By assuming the principal axes of the ellipsoid to be equal, $N(\phi)$ equals , the radius of the earth, and ECEF coordinates on the surface of the earth (x, y, z) is $(Rcos\phi cos\lambda, Rcos\phi sin\lambda, Rsin\phi)$ when altitude equals zero. This is simply the formula transforming for spherical coordinates to Cartesian coordinates.

Since the subject's walking range is small relative to the size of the earth, we approximate the Beekman Park baseball court as a plane tangent to the earth sphere at the trial starting point. Mathematically, ECEF coordinate can be computed to local coordinate by a linear transformation from R^3 to R^3 and transformation can be determined given initial point

geodetic coordinate ϕ_0, λ_0 with local Y axis defined as the vector point to geometrical north, local Z axis defined as the vector from center of earth to starting point, and local X axis as cross product of the Y axis and Z axis. So, we can compute local coordinate of each point as

$$\begin{bmatrix} x' \\ y' \\ z' \end{bmatrix} = \begin{bmatrix} -sin\lambda_0 & \dot{} cos\lambda_0 & 0 \\ -sin\phi_0 cos\lambda_0 & -sin\phi_0 sin\lambda_0 & cos\phi_0 \\ cos\phi_0 cos\lambda_0 & cos\phi_0 sin\lambda_0 & sin\phi_0 \end{bmatrix} \cdot \begin{bmatrix} x - x_0 \\ y - y_0 \\ z - z_0 \end{bmatrix}$$

z' should be very small since we assume altitude equals zero and we get subject's trajectory as the sequence $\{(x_i', y_i'), i = 1,2,3 \ldots\}$ starting from origin. [8] Figure 3 shows the linear transformation schematic.

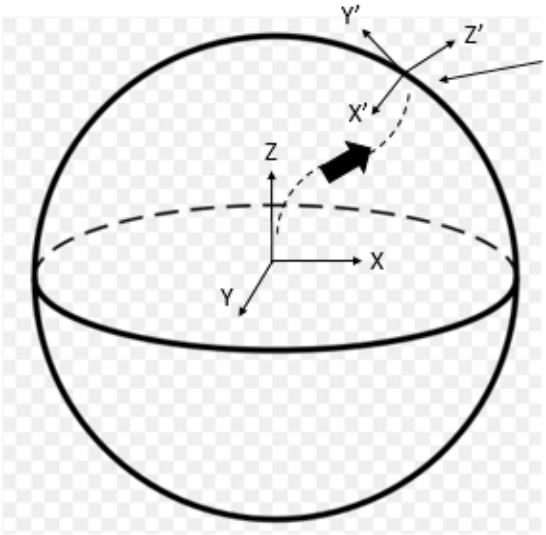

Figure 3: Linear transformation in global coordinate conversion

2.4 Results: Single-sided Ankle Weight

After adding an ankle weight on the leg, we found that the subjects did not show clear tend to walk towards one side. The Figures 4 shows trajectories of all subjects as they have an ankle weight on left foot while Figure 5 shows trajectories of all subjects as they have an ankle weight on the fight foot. As we can see, subjects shifted to the left 5 (out of 8) times as they had an ankle weight on their left ankle, and subject shifted to the right 4 (out of 8 times) as they had an ankle weight on their right ankle. Assuming a null hypothesis that left and right are equally likely, the two-sided p-value of this trial was very close to one meaning that we cannot reject the null hypothesis -- it is valid to believe that the ankle weight does not influence the shifting direction of blindfolded walking.

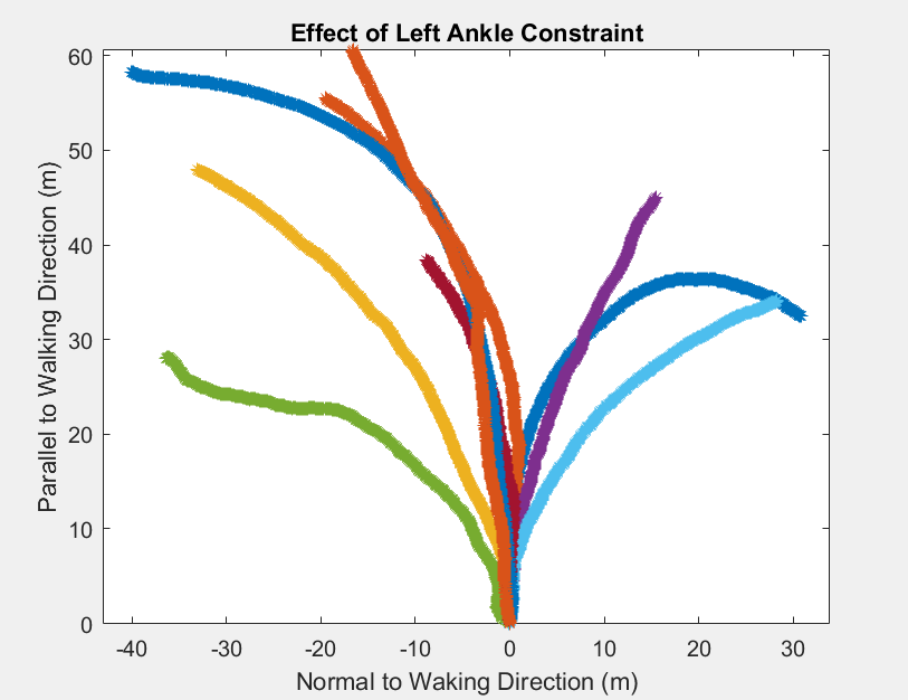

Figure 4: Effect of left ankle weight. This figure shows all the trajectories of left ankle constraint trial conducted by subject 1, 2,3,4,5. Each trial is painted by a unique color.

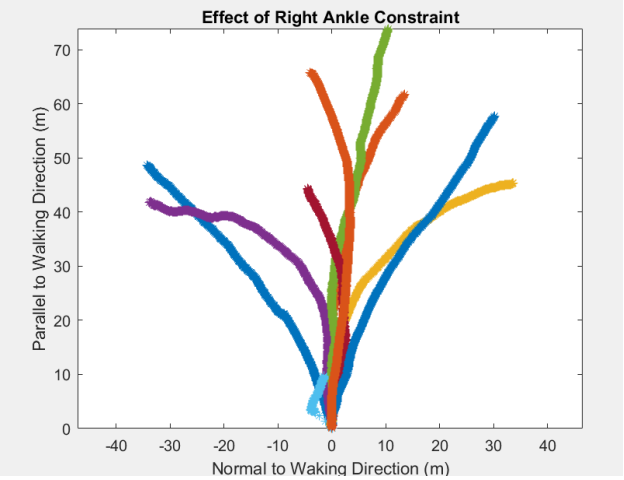

Figure 5: Effect of right ankle weight. This figure shows all the trajectories of right ankle weight trial conducted by subject 1, 2,3,4. Each trial is painted by a unique color.

Moreover, the ankle weight does not have an effect on most of the subject individually. Figures 6, 7 and Tables 2, 3 show the asymmetric ankle weight blindfolded walking trajectories data of subject 1 and subject 2. For subject 1, as this subject has an ankle weight on his left ankle, he shifted to left once and right once. The same happened when the ankle weight was on the right ankle. This means the side of the ankle weight placement is uncorrelated with the blindfolded walking shifting direction.

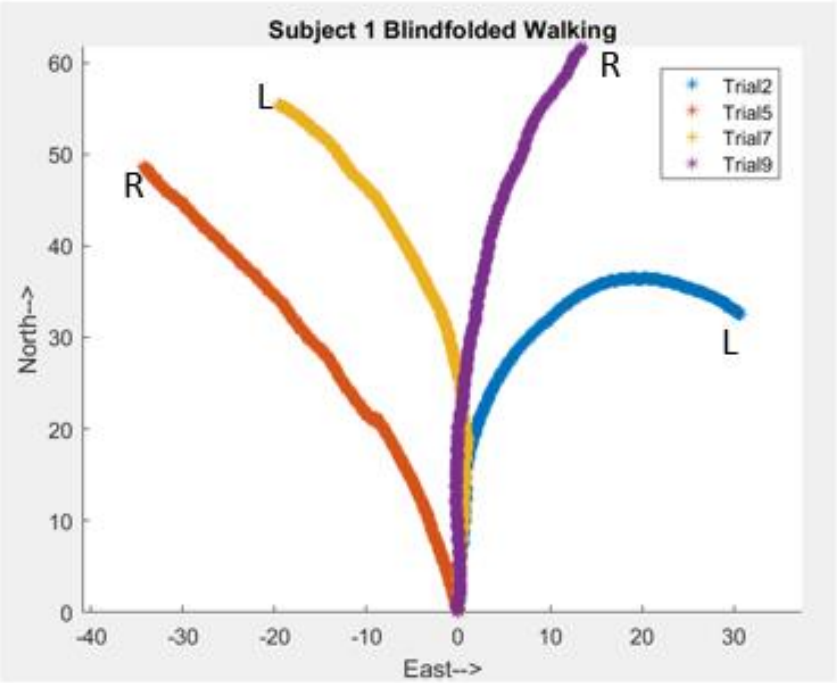

Figure 6: Subject 1 Ankle weight results

To better understand the blindfolded walking trajectory, the set of GPS data curve is least-square-fitted by a portion of the circle of radius, to find the average radius of curvature r. The average angular rate of turn can be computed by the taking the ratio of circle angle and length of trial. It is worth mentioning that the angular rate of turn does not necessarily reflect the shifting direction. Subject may place wider step perpendicular to the walking direction to change the direction of walking.

Table 2: Subject 1 ankle weight data

Constraint	Average angular rate of turn (Rad/s)	Shifting direction
Trial 2 left ankle	-0.0449	Right
Trial 5 right ankle	0.0085	Left
Trial 7 left ankle	0.0207	Left
Trial 9 right ankle	-0.0118	Right

Subject 2 shifted to the left twice (out of 3 trials) as this subject has an ankle weight on the left ankle, and this subject shifted to the right also twice (out of 3 trials) as this subject has an ankle weight on the right ankle. The result was not strong enough to prove that the ankle weight will influence subject's blindfolded walking shifting direction.

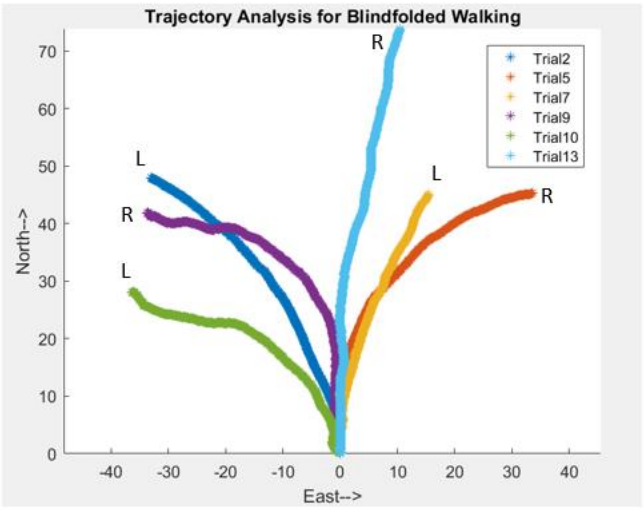

Figure 7: Subject 2 Ankle weight results

Table 3: Subject 2 ankle weight data

Constraint	Average radius of turn (Rad/s)	Shifting direction
Trial 2 left ankle	0.0150	Left
Trial 5 right ankle	-0.0265	Right
Trial 7 left ankle	-0.0085	Right
Trial 9 right ankle	0.0376	Left
Trial 10 left ankle	-0.0087	Right
Trial 13 right ankle	0.0035	Left

2.5 Results: Single-Sided Knee Brace Constraint

We found a systematic trend when subjects had a knee brace on one knee: Subjects shift to the same side where they had a knee brace on. For example, most subjects shifted to the left when they had a left knee brace. Figures 8 and 9 are plots that show the trajectories of the trial that subject has knee brace either on left side or right side. In Figure 8, most of the trajectories show a trend to shift left as a left knee brace was applied. Also, in Figure 9, most of the trajectories show a trend to shift right as a right knee brace was applied. Among 23 knee brace asymmetric walking trials, 17 of trials shift to the side where they had a knee brace on. Two-sided P-value of this trial is under 0.005, and it can be safely concluded that single-sided knee brace influences the blindfolded walking positively.

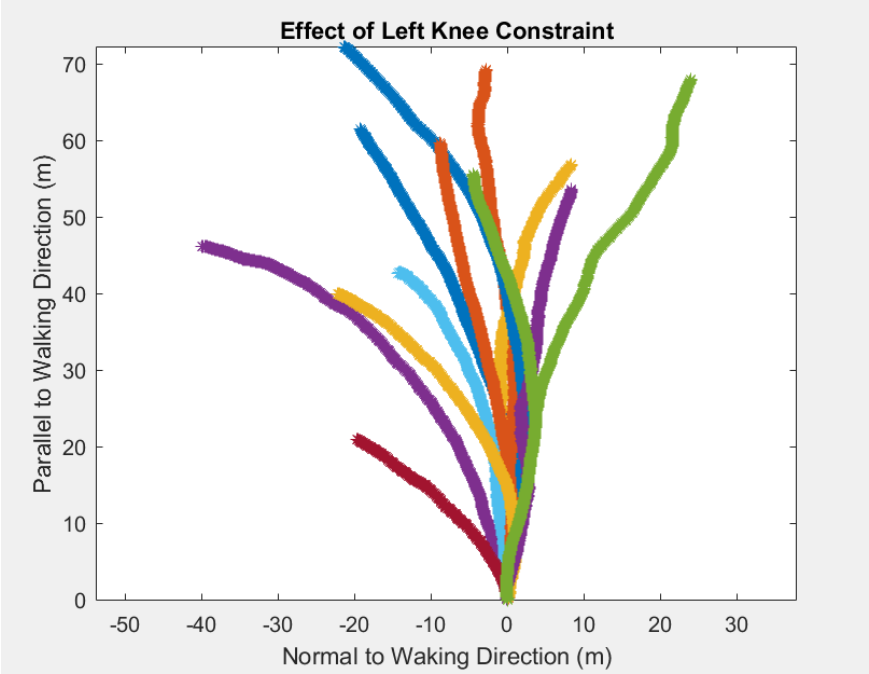

Figure 8: Effect of left knee constraint results. This figure shows all the trajectories of left knee constraint trial conducted by subject 1, 2,3,4,5. Each trial is painted by a unique color.

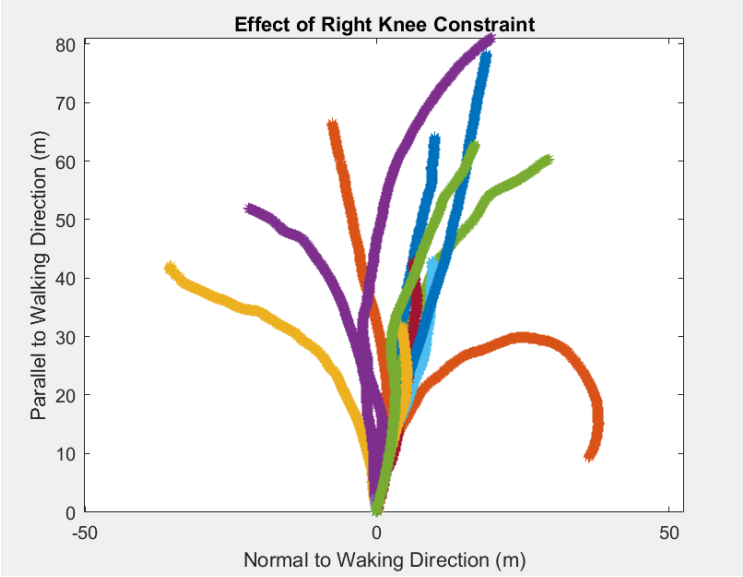

Figure 9: Effect of right knee constraint. This figure shows all the trajectories of right knee constraint trial conducted by subject 1, 2,3,4,5. Each trial is painted by a unique color.

Additionally, knee brace effect affected most of the individual walking pattern. Five subjects (out of 6 subjects) showed a trend to shift to their knee brace side. For example, as shown in Figure 10 and Table 4, subject 1 shifted to the side with a knee brace no matter which side the knee brace was applied.

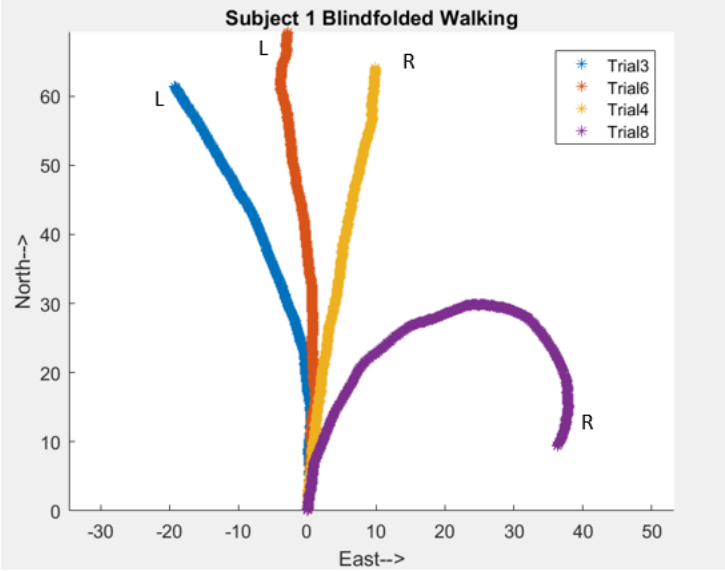

Figure 10: Subject 1 Knee Constraint

Table 4: Subject 1 knee constraint data

Constraint	Average angular rate of turn (Rad/s)	Shifting direction
Trial 3 left knee	0.0122	Left
Trial 6 left knee	-6.1961e-05	Left
Trial 4 right knee	-0.0019	Right
Trial 8 right knee	-0.0688	Right

Same happened for subject 3; This subject shifted to the side with a knee brace no matter which side the knee brace was applied. However, as this subject has a right knee brace, he

tended to shift to the right side by taking wider steps to the right even if subject's average radius of turn is counterclockwise in those two trials.

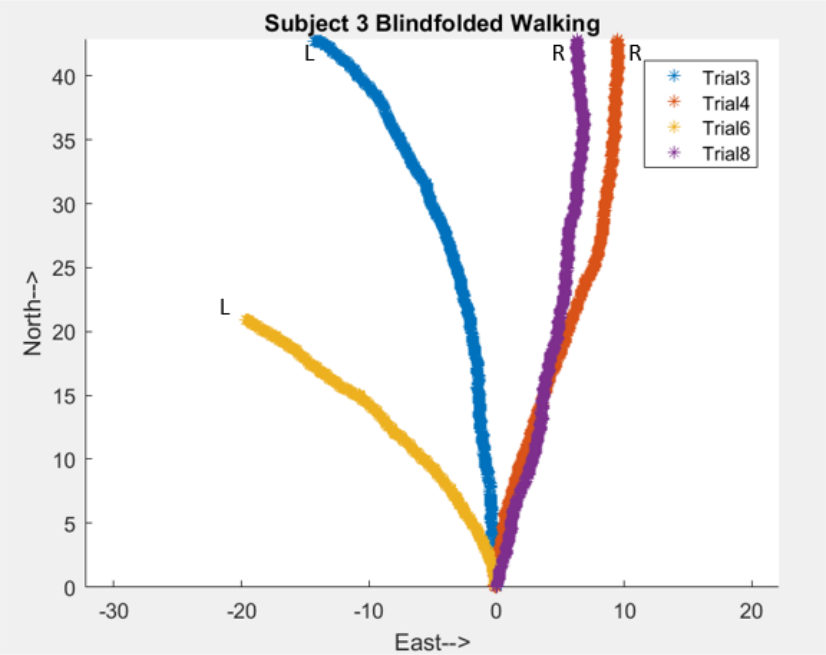

Figure 11: Subject 3 knee constraint result

Table 5: Subject 3 knee constraint data

Constraint	Average radius of turn (Rad/s)	Shifting direction
Trial 3 left knee	0.0155	Left
Trial 6 left knee	0.0075	Left
Trial 4 right knee	0.0159	Right
Trial 8 right knee	0.0057	Right

2.6 Results: Asymmetric Sound Constraint

During the asymmetric sound blindfolded walking experiment, subjects wore a stereo headphone playing “beep” sound on each channel (different beep for each ear). Subjects were instructed to place a step when they heard the beep on the corresponding side’s ear. The beeps for the two sides were not equally spaced in time so that we ask the subjects to step with asymmetric timing. The stride period is defined to be the total time for two complete steps. In Figure 12, $\Delta t_{right}$is defined to be transitional time between placing a left step and a right step. In other words, it also stands for the right foot swing time. The swing time ratio ρ is defined to be the ratio between $\Delta t_{left}/\Delta t_{right}$. Figure 12 shows an example sound profile plot for a trial of length 15 seconds with a stride period of 1.75 seconds and swing time ratio of 0.75. Normal people walk with a swing time ratio around 1, but in our experiment, we set the swing time ratio either between 0 to 1 or above 1 to see whether a difference in swing time will lead to a uniform trend on blindfolded walking trajectory.

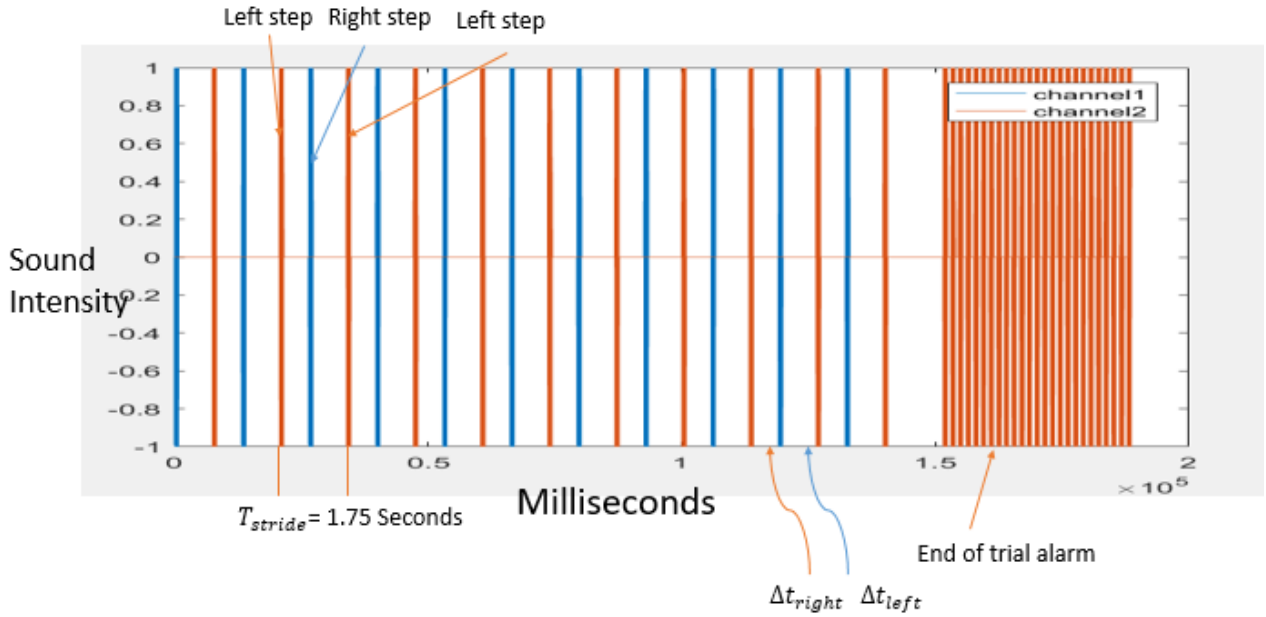

Figure 12: Asymmetric sound profile. Each red "line" is a sinusoid sound wave instructing subject to place a left step. Each blue "line" is a sinusoid sound wave instructing subject to place a right step.

We also define $\alpha := \frac{(\rho)-1}{(\rho)+1}$ to transform the non-linear scale of swing time ratio to a linear scale.

If $\alpha > 0$, then $\rho > 1$ and right leg swing time is lower than the left leg swing time. On the other hand, if $\alpha < 0$, then $0 < \rho < 1$ and right leg swing time is lower than left leg swing time.

In the asymmetric sound constraint experiment, we particularly interested in subjects' average radius of turn rather than general shifting direction because the asymmetric sound controls the swing time of each leg. The turning angle of one walking period can be written as $\theta_{period} = t_{leftswing} \cdot \omega_{left} + t_{rightswing} \cdot \omega_{right}$ where ω is the average angular speed of body turning of placing a left or right step.

The average angular rate of turn of each trial is computed and plotted in Figure 13 along with its corresponding α we defined above. The discrete data set is then fitted by first, second and third order polynomial. As shown in the Figure 13 in the domain of α, all degrees of polynomials have a non-positive derivative. This means that when α is negative, subjects have less left leg swing time than right leg swing time: the average angular rate of turn tends to be positive, implying that they tend to walk counter clockwise, turning to the left. On the other hand, when α is positive, subjects have less right leg swing time than left leg swing time and the average radius of turn tends to be negative and they tend to walk counterclockwise. Secondly, higher asymmetry between two leg swing time, measured by $|\alpha|$ led to higher curvature of the trajectory. Finally, according to the cubic polynomial fit, the curve is flat around origin but not the case as $|\alpha|$ is getting bigger. This means subject will be more susceptible to a change in leg swing time ratio if the asymmetricity is already high.

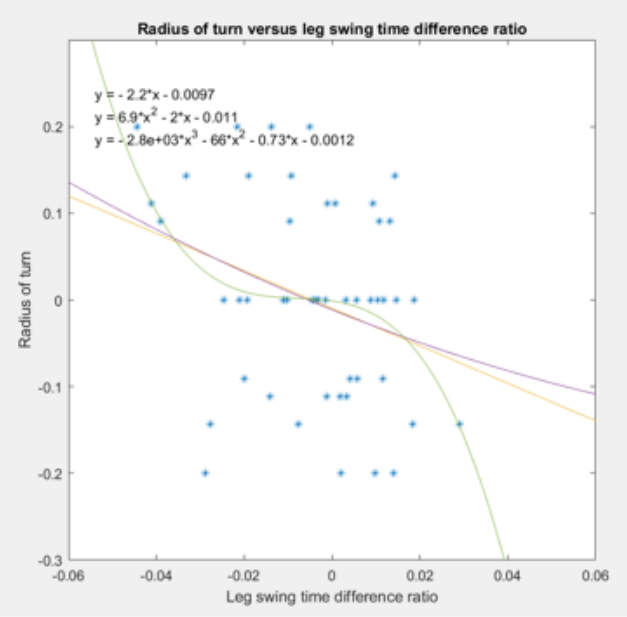

Figure 13: Effect of asymmetric sound (α versus radius of turn).Each dot represents a trial with an α and resultant radius of turn. The figure contains all the trials conducted and the collection of data is fitted by first, second and third polynomials. The fit is not perfect because the great variety observed at $\alpha = 0$ and because the individual different reaction to the asymmetric sound.

We also found that the asymmetric sound affected 3 out of 4 subjects individually. As shown in Figure 14, for subject 7 and subject 8, the polynomial fits have a negative derivative on most of the domain of α and this trend agree with the overall phenomenon.

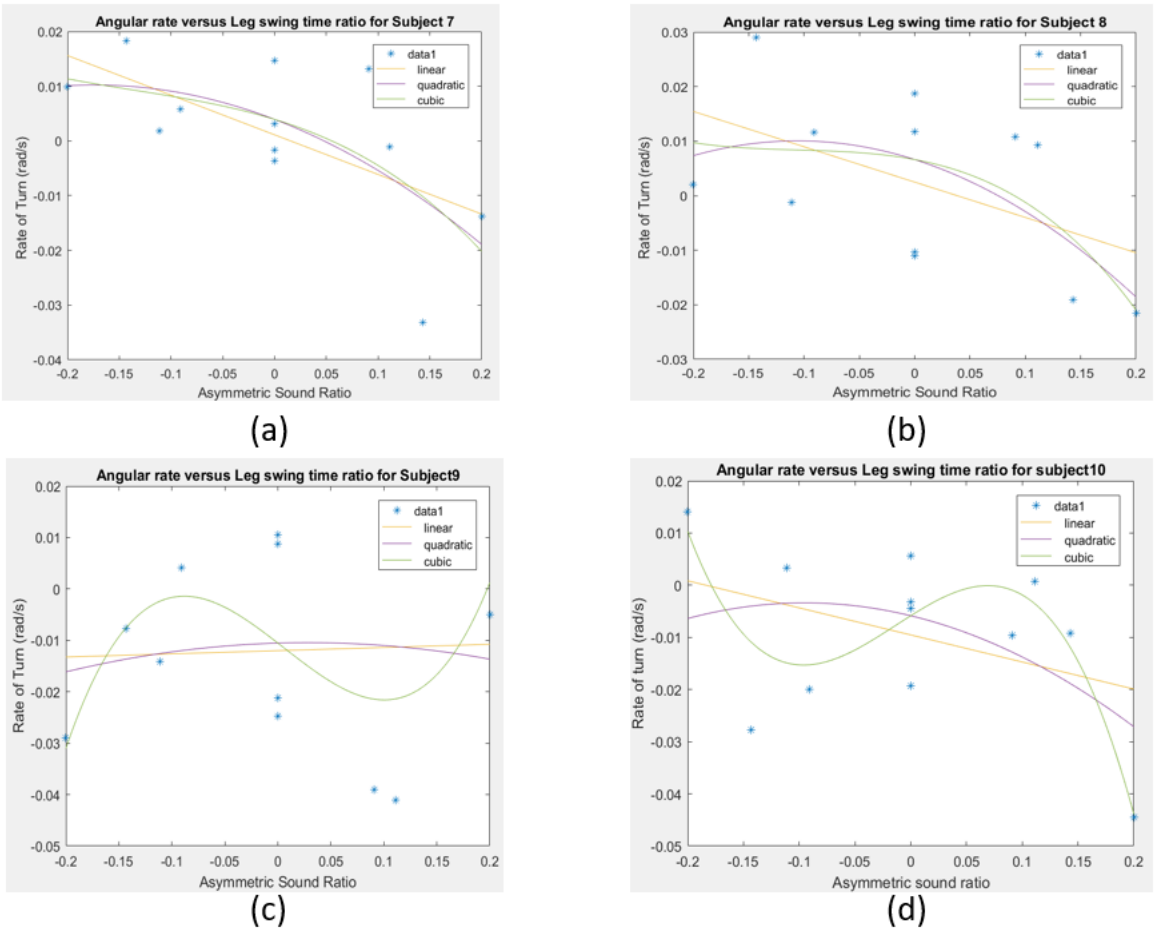

Figure 14: Effect of asymmetric sound on all 4 different subject

a) effect of asymmetric sound on subject 7 b) Effect of asymmetric sound on subject 8 c) Effect of asymmetric sound on subject 9 d) Effect of asymmetric sound on subject 10. Subject 7, 8, 10 's data has a negative slope linear fit, but subject 9 has a slightly positive linear fit. All four subjects have trials that do not follow our general observation, especially for subject 10, resulting a fluctuating cubic fit.

2.7 Conclusion and future work

In the experimental part of this research, we found that difference in single knee stiffness and asymmetric leg swing ratio (imposed using audio) can cause blindfolded walking trajectories to

deviate systematically from a straight line. On the other hand, interestingly, a difference in ankle weight does not have a significant effect --- despite the fact that one of the legs was being "dragged" by the extra weight while the other leg should be easier to swing. One possible explanation for this phenomenon is that subjects' bodies are aware of the fact that one side of the leg is heavier and they try to rectify the situation by applying extra power so that they can walk straight. However, this effort may deviate subjects' normal walking pattern and eventually lead to a more unpredictable result.

There are some places could have been improved in this experimental section so that more definitive and quantitative conclusion can be made. For example, instead of just add an ankle weight, we can vary the specific weight and see if a change in ankle weight can lead to some other result. Further, more "normal" blindfolded walking (without any added asymmetries) should be conducted between the asymmetric blindfolded walking trials so that subject's normal blindfolded walking pattern can be considered before observing the effect of the asymmetric factors.

Chapter 3. A simple mathematical model for blindfolded walking

3.1 Introduction

In the previous chapter, we tried to analyze some asymmetric factors that may affect the blindfolded walking. We found that knee stiffness and leg swing ratio potentially deviate subjects' walking trajectories from a straight line. In this chapter, we explore how individual normal walking pattern may affect their blindfolded walking trajectories.

When we walk, we experience uncertainty factors, for example, uneven terrain, wind and weather or interaction with other people. These uncertainty factors contribute to the perturbation of our body, and our body will react to this perturbation to keep balance and walk efficiently. Everyone has their unique physique (leg length, muscle development, the center of gravity) as well as strategies to keep balance and optimize energy consumption, which lead to a unique walking pattern. This walking pattern may be different in different situations and depends on the individual's purpose. For example, most of us walk similarly on the treadmill because we have a specific purpose: walking straight and our vision can prevent us from walking out of the band and getting injured. However, as we do blindfolded walking, vision is blocked, and the trajectories of blindfolded walking can tell us a lot about our walking pattern and the reaction towards the perturbation.

If we know the walking pattern, then blindfolded walking trajectories on a simple terrain may perhaps be predicted. In this chapter, we analyze big normal treadmill walking data from 10 subjects and learn how each subject turn their body and place steps given certain perturbation

condition. Then, we generate a set of walking trajectories according to their walking pattern through a random iterative process for each subject.

3.2 Mathematical model construction

In the simulation, the human body is simplified as a three-point model as shown in Figure 15. The pelvis point on the top is a mass point representing the entire upper body above the leg. Two points at the bottom represent two feet, and vertices connecting pelvis point represent two legs.

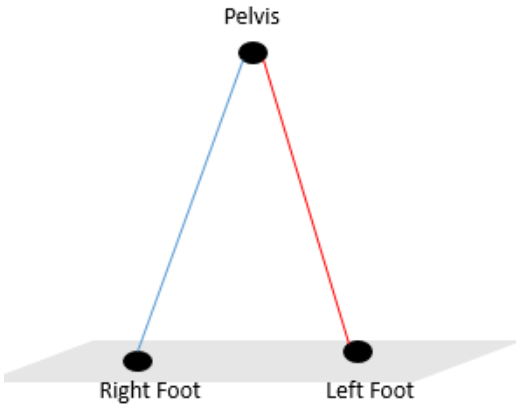

Figure 15: 3-point walking model

The entire bipedal walking gait cycle includes six phases about each leg: Heel Strike (HS), Foot Flat (FF), Mid-Stance (MS), Heel-Off (HO), Toe-Off (TO), and Mid-Swing (MS). Figure 16 demonstrates the gait cycle about both legs with the abbreviation of each phase marked.

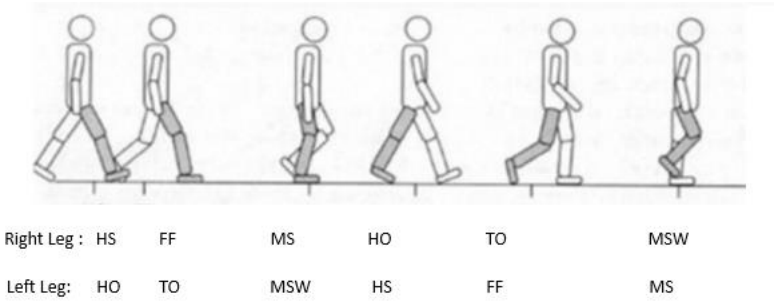

Figure 16: Human walking gait cycle [10]

Since we simplified human body as a three-point model, gait cycle can be simplified as shown in Figure 17. Heel Strike and Foot Flat phases are combined as one Foot Step phase while Heel Off and Toe Off phase is the Foot Step phase of the other leg. We will use the simplified gait cycle phase shown in Figure 17 for the rest of analysis.

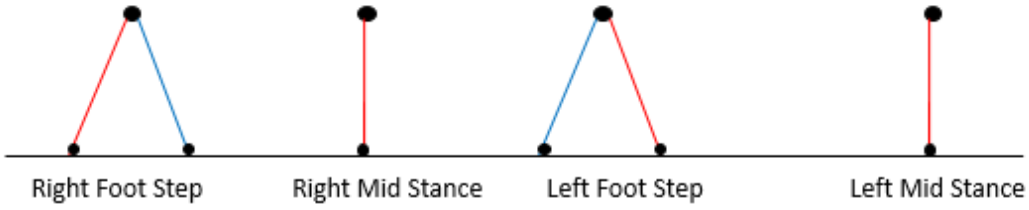

Figure 17: Simplified gait cycle

Treadmill walking data used in this chapter were previously collected by the Ohio State University Movement Lab [9]. Subjects wear three markers at torso and three markers on each foot as shown in Figure 18.

Figure 18: Marker placement demonstration [2]

As subjects were walking on the treadmill, Vicon T20 Motion Capture Camera at 100 Hz recorded the positions of each marker in 3D (x-y-z). Pelvis point coordinate in the three-point model is calculated by taking the average of coordinates of 3 markers at torso position and foot point in the three-point model is calculated by taking the average of the coordinates of 3 markers on each shoe. We can construct our three-point model in Matlab from motion capture camera data as shown in Figure 19. We use the following convention: x is the rightward direction, y is the forward direction, and z is the upward vertical direction.

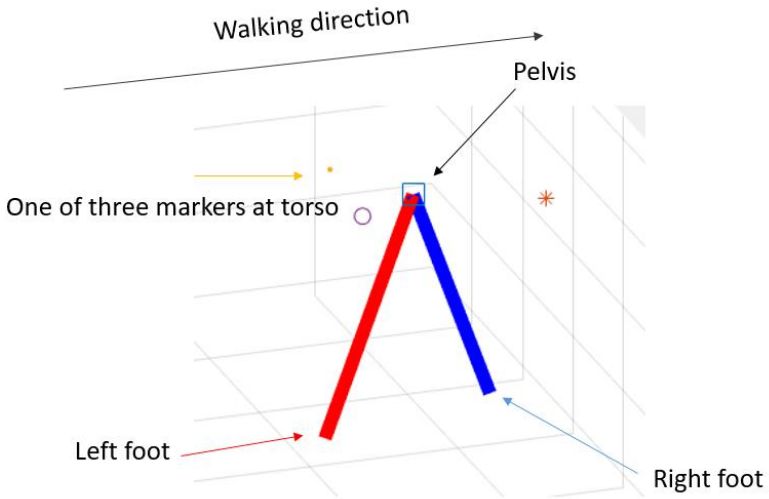

Figure 19: Construction of 3-point walking model. An example position of the 3 points from the walking data.

3.3 Data Processing

Let us define $\mathcal{p}(t)$ from $R \to R^3$ as pelvis position function with respect to time and $\mathcal{f}_l(t)$,$\mathcal{f}_r(t)$ from $R \to R^3$as left foot and right position function with respect to time. Motion capture camera then takes data at a 100 Hz sampling rate and this discrete data set can approximate our model's continuous walking reasonably and give us a clear picture of each walking phase defined in last section.

We define left foot stepping phase happens at the moment when left foot markers reach the lowest point on z coordinate. To obtain the set t_{LS}, we use 'findpeak' function on $-\mathcal{f}_l|_z(t)$, the z coordinate of the left foot. To get the Left Foot Stepping phase time t_{LS}at each gait cycle period T_{gait}, we take

$$t_{LS} = \not{f}_l^{-1}(MIN(\not{f}_l|_z(T_{cycle})))$$

where T_{cycle} is the set of discrete time captured by motion capture camera for all complete T_{gait}.

Similarly, we determine the right foot stepping phase as follows: take $t_{RS} = \not{f}_r^{-1}(MIN(\not{f}_r|_z(T_{cycle})))$ and use 'findpeak' function on $-\not{f}_r|_z(t)$, the right foot z coordinate. The Figure 20 shows the left and right stepping moment extracted among all data points.

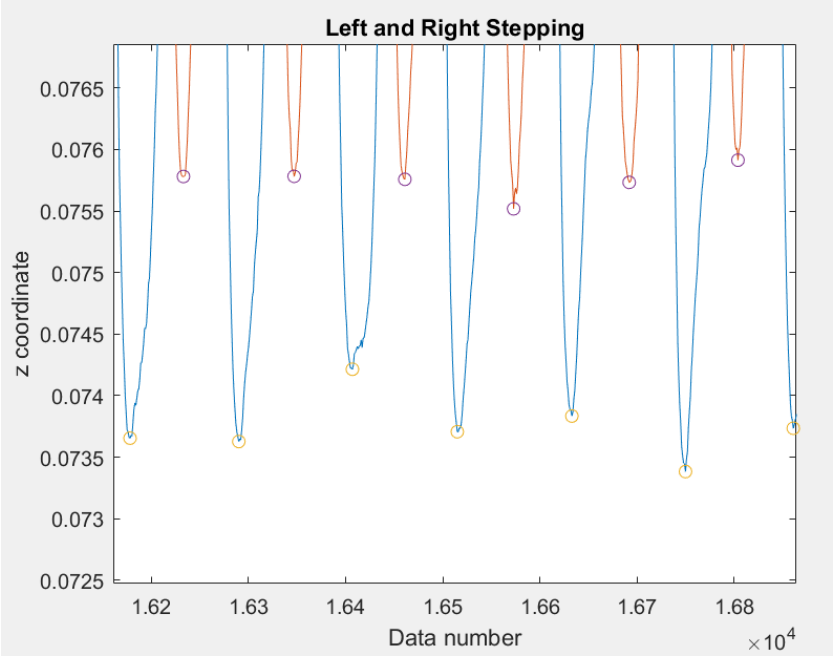

Figure 20: Stepping points collection. Left and right stepping phase moment for subject 3 Trial1, obtained as the minima of their feet's z coordinate.

There is a small difference between the minimum left and right stepping z coordinate due to marker placement on each shoe. The difference is around 0.001 meter, which is ignorable relative to subject's height and stepping length.

After we get the set of t_{LS} and t_{RS}, we can get stepping coordinate on the xy-plane by: $\not{f}_l|_{x,y}(t_{LS})$ and $\not{f}_r|_{x,y}(t_{RS})$ and corresponding standing leg coordinate as $\not{f}_r|_{x,y}(t_{LS})$ and $\not{f}_l|_{x,y}(t_{RS})$. Figure 21 shows all the stepping points and standing points within a walking trial.

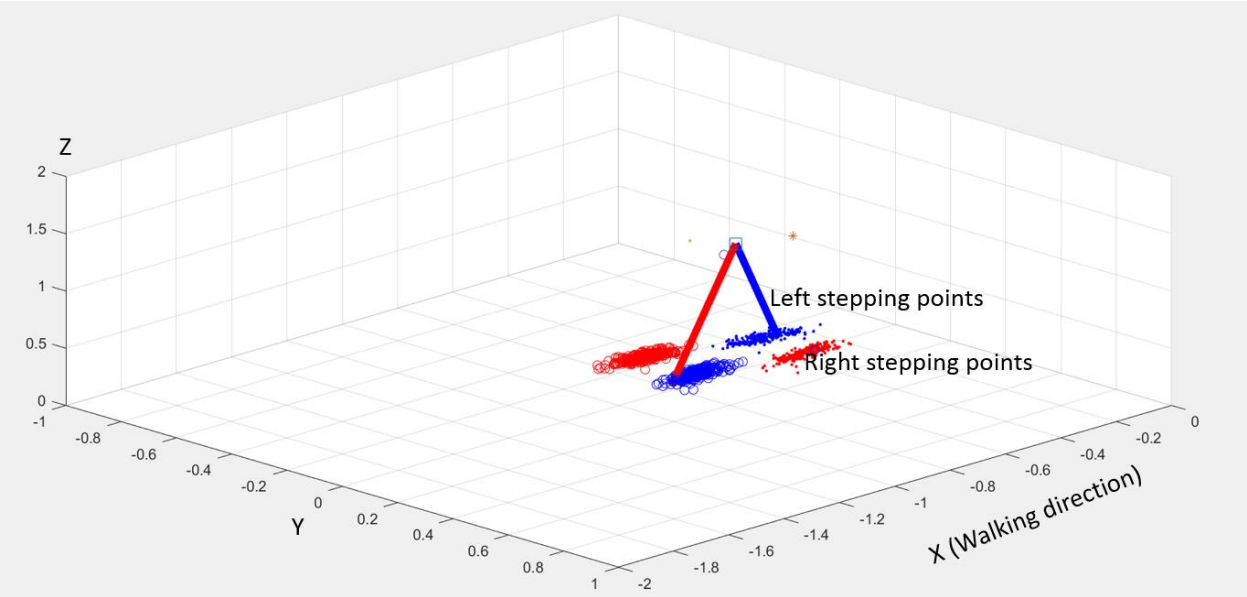

Figure 21: Left and right stepping point and corresponding "standing" point relative to the lab frame.

However, it is worth mentioning that standing point is the "Heel OFF" phase coordinate as shown in Figure 22. Since we only consider x,y coordinate in the later simulation, we can approximate these slightly elevated points as standing points.

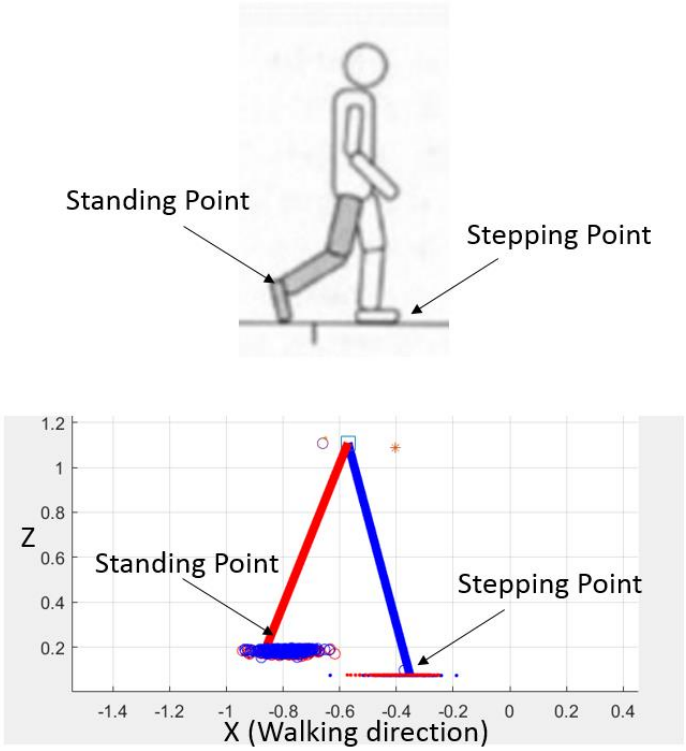

Figure 22: Side view of heel off phase

Finally, we get a vector from standing point to stepping point by subtracting the x, y coordinate of stepping point by standing point coordinate, treating the standing point as origin. Figure 23 shows the relative stepping point for a single trial. As we can see, the stepping points for either left foot or right foot are stochastic, but stepping locations can roughly tell us the mean stepping position and its standard deviation. In the next step, we will match this relative placement by mid stance perturbation by a regression [9].

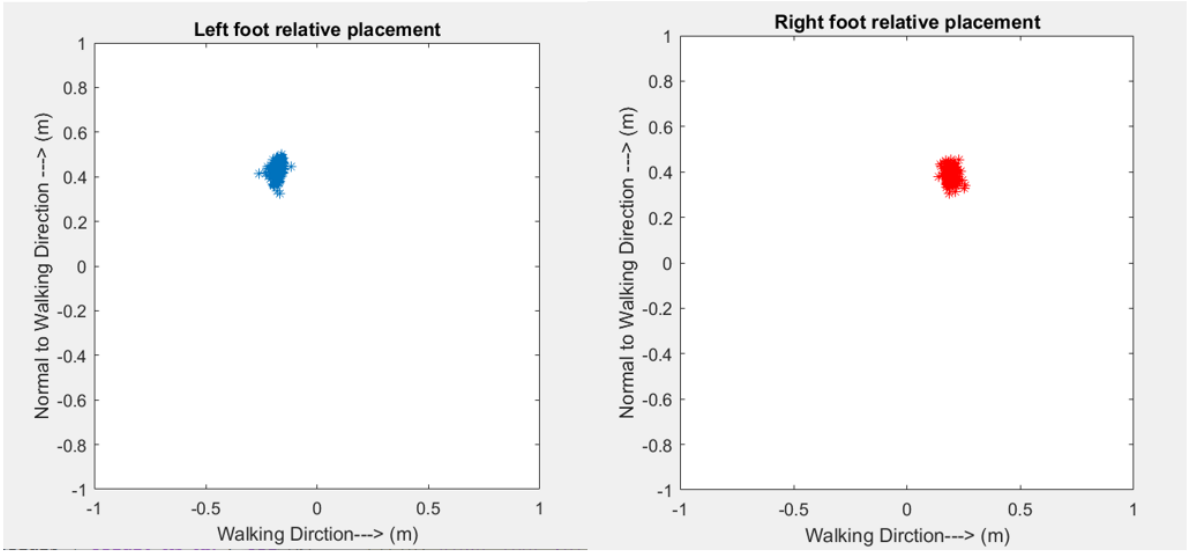

Figure 23: Relative foot placement. Left foot placement relative to the previous right foot represented by (0,0) and vice versa.

To evaluate the perturbation during walking, we first find the mid-stance moments t_{MS} during each gait cycle. Let us define a half gait cycle $T_{halfcycle}$ as the time period between any consecutive left stepping and right stepping phase. We take

$$t_{MS} = \mathcal{p}^{-1}(MAX(\mathcal{p}|_z(T_{halfcycle})))$$

Simply saying, we define that the mid-stance phase happens when the y coordinate of the pelvis point reach its maximum between each consecutive left step phase and right step phase. In the Matlab, we use 'findpeak' function to find the maximum of $\mathcal{p}_y(t)$ within each $T_{halfcycle}$. The Figure 24 shows the mid-stance moment extracted from the pelvis y coordinate data.

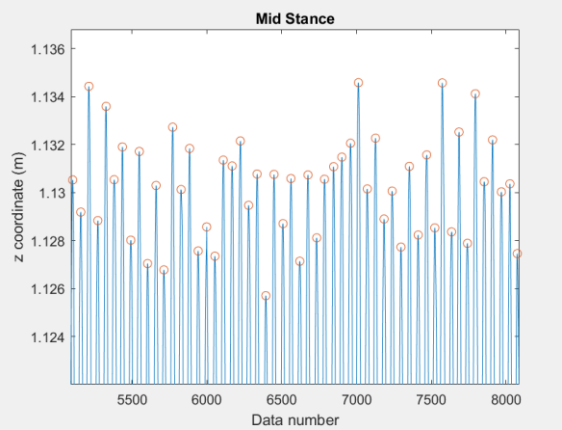

Figure 24: Extracted mid stance moments denoted by circles for subject 3 Trial1, defined as the maximum of the pelvis z coordinates.

The z coordinate of the mid-stance varies slightly at each mid stance moment (Figure 24) because as one leg swing pass another, the distance between two feet varies leading to a various mid-stance pelvis height.

Heading angle is the direction of walking. For the normal treadmill walking, the heading angle varies very little because people must stay on the walking band. However, we found our body experience a small heading angle change before and after mid-stance phase to keep the body stable from the perturbation effect and to place next step. Heading angle can be calculated by tracking the change of vector angle defined by three torso markers.

As shown in Figure 25, let $\mathcal{T}_{1,2,3}$ be three marker positions on torso and m is the midpoint of marker $\mathcal{T}_1$ and $\mathcal{T}_2$. Let us define the heading angle vector $u \coloneqq \overrightarrow{m\mathcal{T}_3}$ and a change of heading angle after mid stance position is the angle between u and u' where u is heading angle vector a 0.2s before mid-stance moment and u' is the heading angle vector 0.2 s after mid-stance moment.

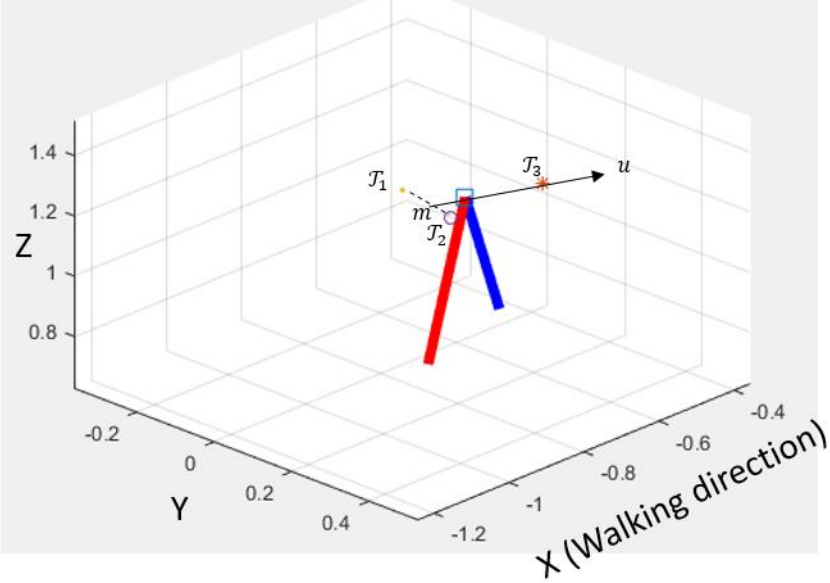

Figure 25: Heading angle vector

Figure 26 plots the heading angle change in a trial. As we can see, the change of heading angle is very small but distributed quite evenly above and below zero. This is because placing left or right step will normally lead to a change in heading angle of different sign.

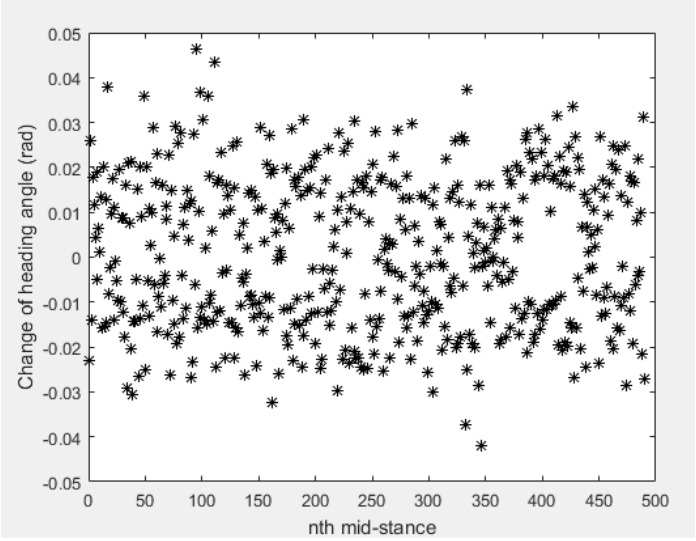

Figure 26: Change of heading angle distribution for subject 3 Trial1

During blindfolded walking, perturbations due to various reasons so that there is step-to-step variability in the pelvis point may be one of the major reasons of unpredictable trajectories outcome. Perturbation means the deviation from the normal state. Here, the perturbation means the pelvis point position and velocity deviation from ideal gait cycle. As people walking on the treadmill, their walking speed plus treadmill speed equals zero leading to an ideally still pelvis point at mid-stance. But this does not happen because we experience perturbation inevitably during all walking condition.

Deviation of the pelvis point at mid stance moment can be calculated by comparing current mid stance pelvis position coordinate with the mean mid stance pelvis coordinate. Figure 27 shows the position perturbation distribution from a walking trial.

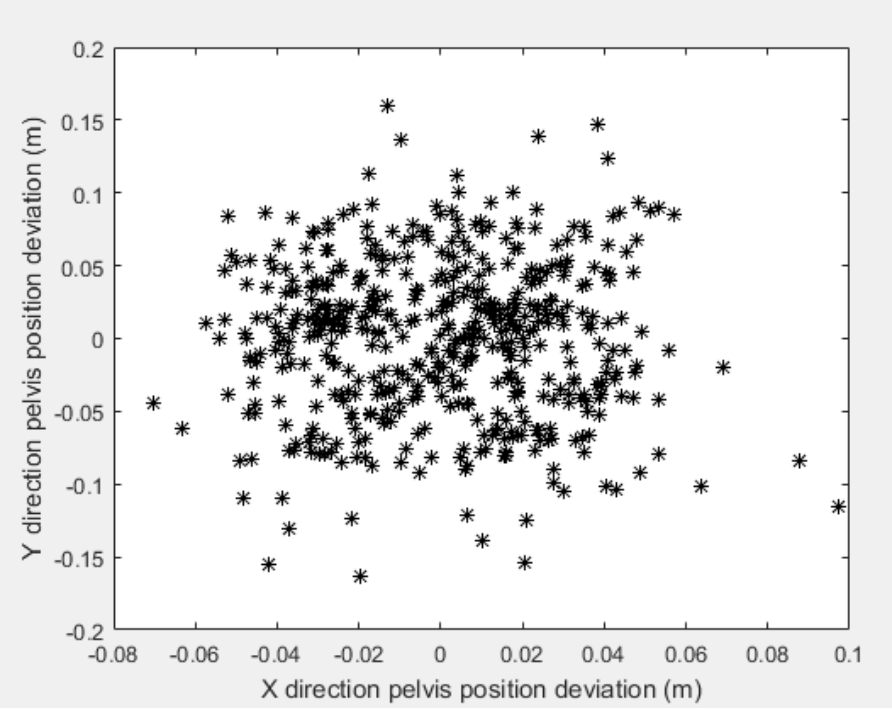

Figure 27: Pelvis position perturbation distribution for subject 3 Trial1

Velocity deviation at the pelvis point can be calculated by

$$v_x = \frac{d\mathcal{p}_x(t)}{dt}|_{t_{midstance}} \approx \frac{\mathcal{p}_x(t_{midstance} + \Delta t) - \mathcal{p}_x(t_{midstance} - \Delta t)}{2\Delta t}$$

$$v_y = \frac{d\mathcal{p}_y(t)}{dt}|_{t_{midstance}} \approx \frac{\mathcal{p}_y(t_{midstance} + \Delta t) - \mathcal{p}_y(t_{midstance} - \Delta t)}{2\Delta t}$$

Figure 28 is a plot of v_x versus v_y for a single trial

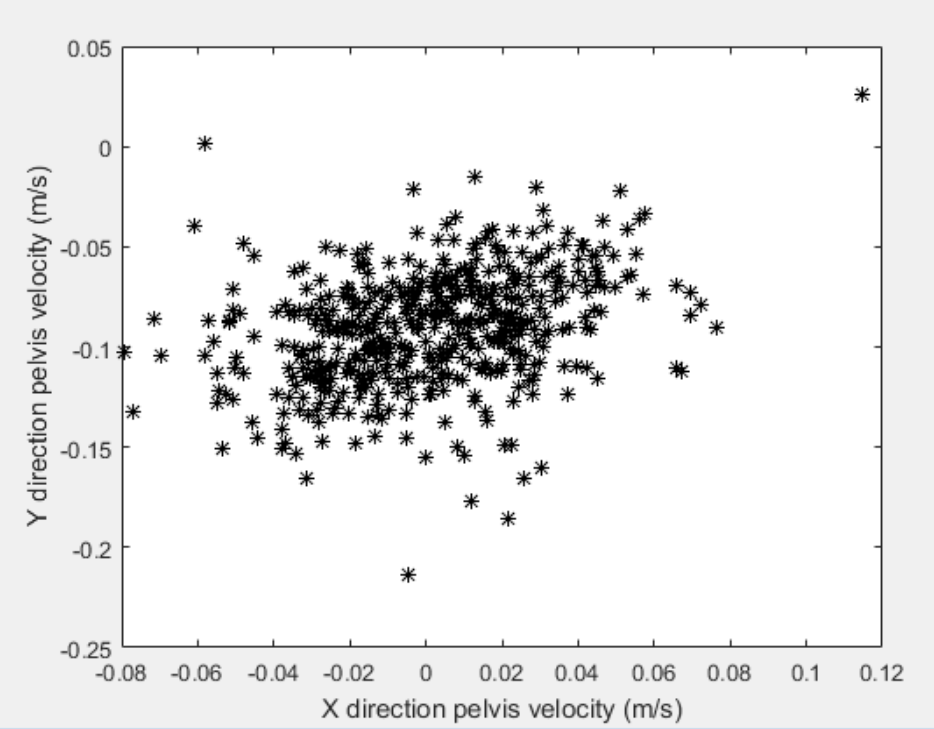

Figure 28: Velocity perturbation distribution for subject 3 Trial1

The data explained above can be separated by left action and right action. For example, the perturbation velocity can be separated by left perturbation velocity and right perturbation velocity according to which step (left or right) the subject is about to step.

In the case of change of heading angle, data can be separated mostly by $y = 0$. However, how left and right perturbation data is distributed within Figure 28 is a lot more convoluted and profoundly affects the final simulated trajectories. Since left steps and right steps was simulated alternatively as we generate the blindfolded trajectories, we will categorize all the data presented above by left and right so that the simulation process can be more realistic.

3.4 Multivariate linear regression to obtain step-to-step mapping

To generate a blindfolded walking trajectory, it is essential to know how subjects place a step after mid-stance phase given a certain direction and what direction subjects face at each mid-stance phase. On the other hand, these values are related to subjects' walking patterns at the presence of perturbation.

To generate a trajectory, we need a sequence of perturbation data $\{(\Delta x, \Delta y, v_x, v_y)\}_i$ and four transformation matrices$M_{step,left}$, $M_{step,right}$, $M_{angle,left}$ and $M_{angle,right}$ so that

$$\begin{pmatrix} \Delta x_{step} \\ \Delta y_{step} \end{pmatrix}_{left} = M_{step,left} \cdot (\Delta x, \Delta y, v_x, v_y)^T$$

$$\begin{pmatrix} \Delta x_{step} \\ \Delta y_{step} \end{pmatrix}_{left} = M_{step,right} \cdot (\Delta x, \Delta y, v_x, v_y)^T$$

$$\theta_{left} = M_{angle,left} \cdot (\Delta x, \Delta y, v_x, v_y)^T$$

$$\theta_{right} = M_{angle,right} \cdot (\Delta x, \Delta y, v_x, v_y)^T$$

The easiest way to get these matrices is to do multivariate linear regression between subjects' normal walking perturbation and its corresponding change of heading angle and stepping

coordinate. Since we can collect all perturbation and walking data from the last section, we just need to use Matlab function 'mvregress' to get the matrices. These four matrices carry the most information about subjects' walking patterns, and we will use these matrices to generate a sequence of blindfolded walking trajectories.

There are papers analyzing the properties of matrix M and how different healthy people share a similar M_{step}. For example, in Yang Wang and Manoj Srinivasan's paper "Stepping in the direction of the fall: the next foot placement can be predicted from current upper body state in steady-state walking", they found that ΔX_{step} is positively related to Δx and v_x while ΔY_{step} is negatively related to Δx and v_x.[9]

Here, we pay more attention to the uniqueness of these matrices, and we focus on the personal difference between the behavior of left stepping pattern and right stepping pattern. For example, the width of left stepping pattern and right stepping pattern are relatively similar for subject 2 ($\Delta x_{step,right} \approx 0.2754\Delta x + 0.1978v_x, \Delta x_{step,left} \approx 0.2499\Delta x + 0.2623v_x$). Both of them depends positively on the position deviation and velocity perturbation. However, the length of the stepping on each side differs quite a lot, especially on the reaction of x direction perturbation. ($\Delta y_{step,right} = -0.8765\Delta x + 0.0960\Delta y - 1.0142v_x + 0.4726v_y, \Delta y_{step,left} = 1.3912\Delta x + 0.0880\Delta y - 1.8295v_x + 0.6606v_y$)

On the other hand, different from subject 2, subject 5's left stepping pattern is less dependent on Δx, but right stepping pattern depends on Δx just like subject 2. ($\Delta x_{step,right} \approx 0.1306\Delta x + 0.1465v_x,\ \Delta x_{step,left} \approx -0.0701\Delta x + 0.1697v_x$).

The right heading angle of subject 5 may be predicted by $\Delta\theta_{right} = 0.0732\Delta x + 0.0198\Delta y + 0.0449v_x + 0.07v_y$ while $\Delta\theta_{left} = 0.911\Delta x - 0.2458\Delta y - 4.0591v_x + 0.6808v_y$. From the sign and magnitude of the factors, we can see that subject 5 usually face right when placing a right step while facing left when placing a left step given a small perturbation, but x direction velocity perturbation affect how much he or she turns more when placing a left step.

3.5 Simulation algorithm

To best simulate the each subjects' blindfolded walking, it is necessary to include both the random factors and individual walking behavior. Let us assume subject experience normally distributed perturbation in pelvis state $(\Delta x, \Delta y, v_x, v_y)$ at every mid-stance phase where

$$\Delta x \sim N(\mu(\Delta x^*), var(\Delta x^*)),$$

$$\Delta y \sim N(\mu(\Delta y^*), var(\Delta y^*)),$$

$$v_x \sim N(\mu(v_x^*), var(v_x^*)),$$

$$v_y \sim N(\mu(v_y^*), var(v_y^*)),$$

The variables with a star superscript came from normal treadmill walking data. Then the distribution of stepping coordinates and change of heading angle follow the distributions transformed by matrix M_{step} and M_{angle}.

$$\begin{pmatrix}\Delta x_{step}\\ \Delta y_{step}\end{pmatrix} \sim N(\mu(M_{step} \cdot (\Delta x^*, \Delta y^*, v_x^*, v_y^*)^T), var(M_{step} \cdot (\Delta x^*, \Delta y^*, v_x^*, v_y^*))^T)$$

$$\theta \sim N(\mu(M_{step} \cdot (\Delta x^*, \Delta y^*, v_x^*, v_y^*)^T), var(M_{step} \cdot (\Delta x^*, \Delta y^*, v_x^*, v_y^*))^T)$$

Mean of $\begin{pmatrix}\Delta x_{step}\\ \Delta y_{step}\end{pmatrix}, \theta$ can be calculated by the linearity property of μ, while variance of $\Delta x_{step}, \Delta y_{step}$is calculated by:

$$var\left(\Delta x_{step}\right) = var\left(M(1,1)\Delta x^{*} + M(1,2)\Delta y^{*} + M(1,3)v_x + M(1,4)v_y\right)$$

Variances of linear combinations of two or more variables can be obtained using $var(aX + bY) = a^2 var(X) + b^2 var(Y) + 2ab \cdot covar(X, Y)$ and $covar(X, Y) = E(XY) - E(X)E(Y)$. We have a similar calculation for θ. Of course, for all such statistical operations, we simply use MATLAB's in-built functions.

As shown in the derivation, given a perturbation distribution, every turning and stepping after mid-stance are stochastic. Therefore, a sequence of perturbation will result in a sequence of turning and stepping, which suffice to form a trajectory. Figure 29 demonstrates the algorithm of blindfolded walking simulation. At mid-stance (including the initial standing phase), we give our three-point model a perturbation and result in a left or right stepping location, and we rotate the coordinate system by its change of heading angle, and then, the model will swing right or left leg and go to mid-stance phase again. Again, we give the mid-stance phase model a perturbation, which results in a right or left stepping. This process goes on for the duration we define, and the trajectory is just the set of coordinates of each stepping location.

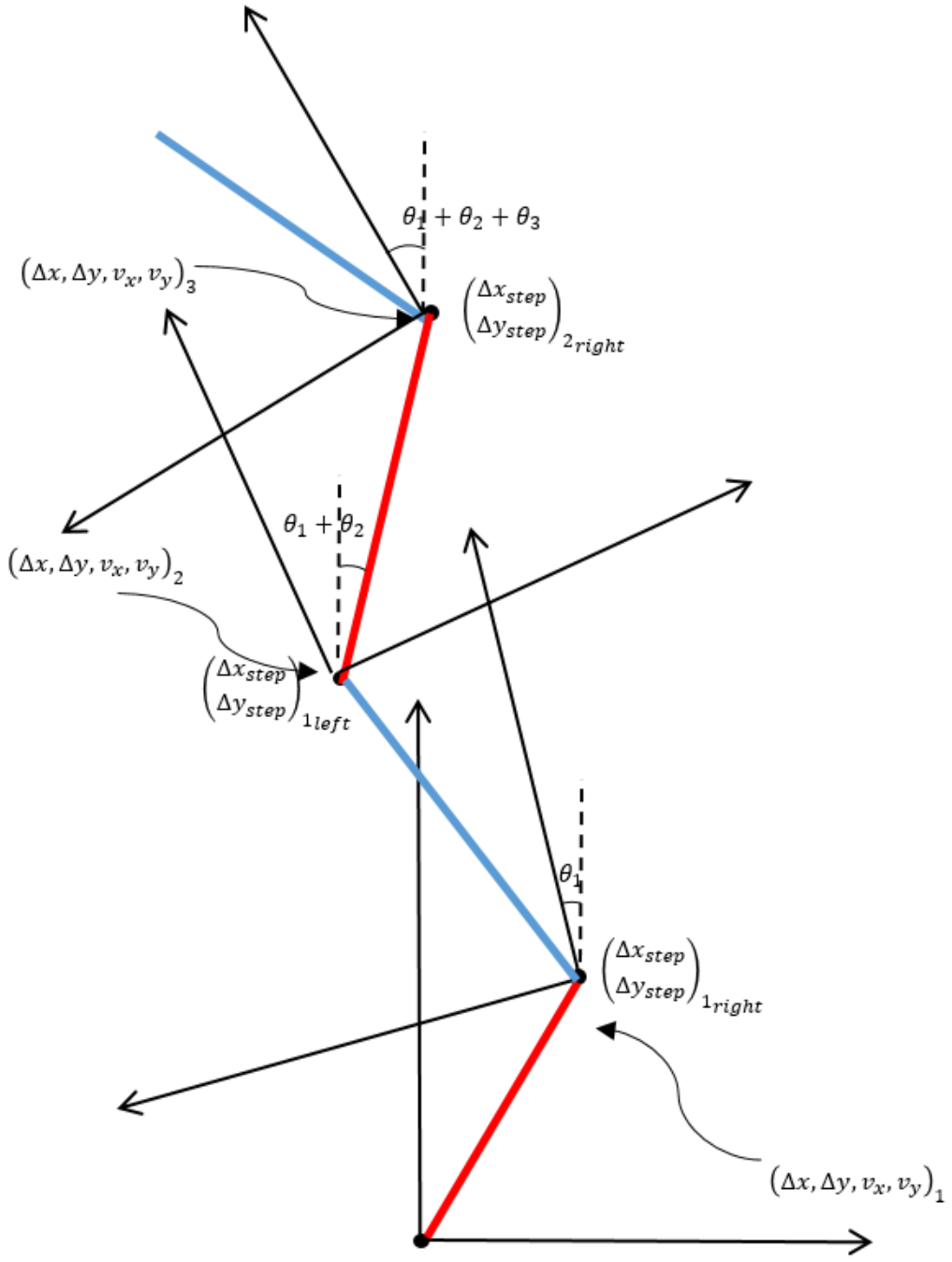

Figure 29: Simulation algorithm: A red line indicates a left to right step and a blue line indicates a right to left step. The 'local' body-fixed coordinate frame is shown with black arrows, with the sideways coordinate axis pointing left or right based on whether the next step is left or right.

3.6 Simulation results, observation, and evaluation

Having obtained this linear step-to-step model with step-to-step mid-stance perturbation, we simulate this mathematical model for each subject separately for a duration of 70 gait cycles. Figure 30 shows the result of a simulation for subject 3.Every star is a left step point, and every circle is a right stepping.

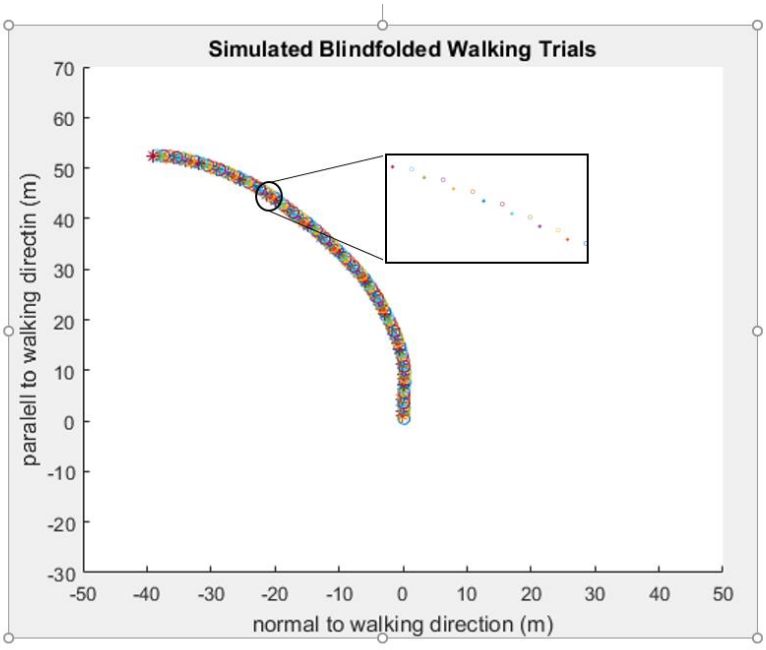

Figure 30: A sample trial for subject 3

The result shows consistency among each trial. As shown in Figure 31, 5 trials were simulated and they all shifted to the left with similar trajectories. The five trajectories are slightly different because this is a stochastic model, with noise perturbation added to the pelvis state at every mid-stance.

Figure 31: 3 Sample trials for subject 3

However, for different subjects, the results show great difference due to the different walking pattern. As shown in Figure 32, we took mid-point of each left and right stepping point and got new single-line trajectory. As we can see, all four subjects show great individual features. We found that subjects usually go straighter in the simulation if they take larger steps while subjects who take smaller steps will usually shift to one side very quick or even go around the circle.

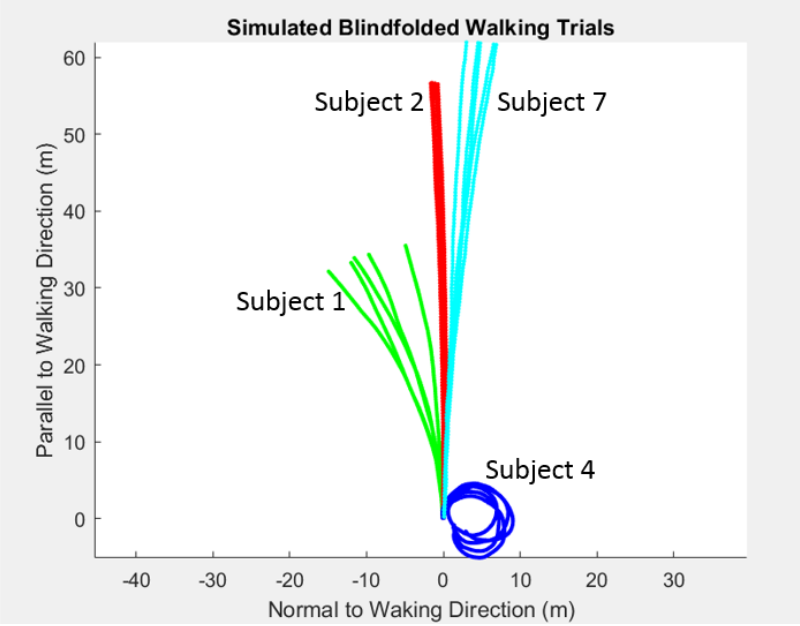

Figure 32: Simulated trials for four subjects

An interesting fact is that, as the duration of the trial goes up, subject will eventually go around in an approximate circle since in the data, the noisy deviations of heading angle before and after mid-stance distributed evenly around zero, but we obtain a biased random walk if the mean θ change per step giving rise to a systematically biased random walk (which is why the model shifts systematically one way or the other). Since our simulation is an iterative process, by random walk theory,

$$\theta_{total} = \sum \theta_i$$

$$E(\theta_{total}) = \sum E(\theta_i) = n\mu(\theta^*)$$

Eventually, $|\theta_{total}|$is expected to go out of bounds, meaning the subject would go around circle for some finite number of steps. The Figure 33 shows a simulated trial for a length of 1000 gait cycles for subject 3.

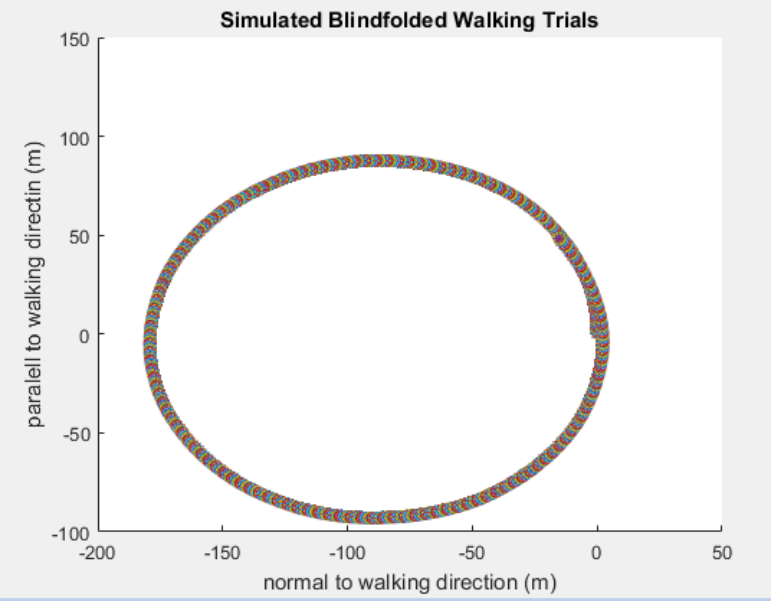

Figure 33: 1000 gait cycles simulation for subject 3

The derivation above also implied the prediction of Bestaven et al [3]. As walking blindfolded or walking at a place without landmarks, people may walk around circles and get lost. From our simulation, this circular walking behavior can be explained by not only the postural asymmetry but also, their walking behavior and response to perturbation.

3.7 Future work

Since the simulation is just a predicted blindfolded walking trajectory and is based on non-blindfolded data, we want to let the subject do the actual blindfolded walking (without constraint) and see if the experimental results converge with the simulation. The data used to derive this probabilistic model was different from a different set of subjects (from 5 years ago) than the subjects used in our blindfolded experiments. It would be good to have the same set of subjects.

Additionally, aside from using multivariate regression to learn subjects' walking patterns, more advanced technique can be used to do the learning. We observed that subjects with "separable" behavior tend not to walk straight. For example, as shown in Figure 34, some subjects experienced relative uniformly distributed perturbation while others experienced biased and separable perturbation cluster at mid-stance depending on whether they are about to place a left step or a right step. However, we need a more advanced tool to justify this hypothesis.

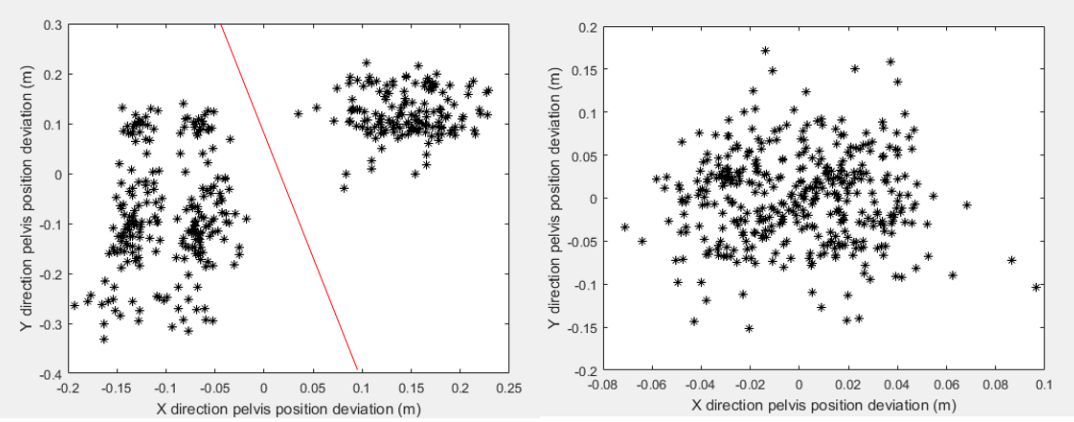

Figure 34: Separable position perturbation versus uniform position perturbation

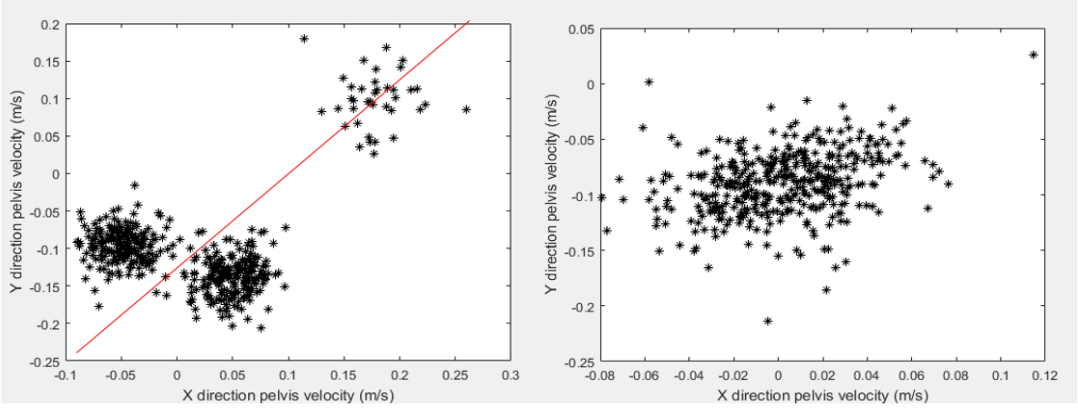

Figure 35: Separable velocity perturbation versus uniform velocity perturbation

Also, as shown in Figure 36, we also found that after mid-stance phase, some subjects tend to change heading angle rapidly between left and right stepping while some other subjects may only change heading angle slightly. Those who change heading angle rapidly tend not to walk straight.

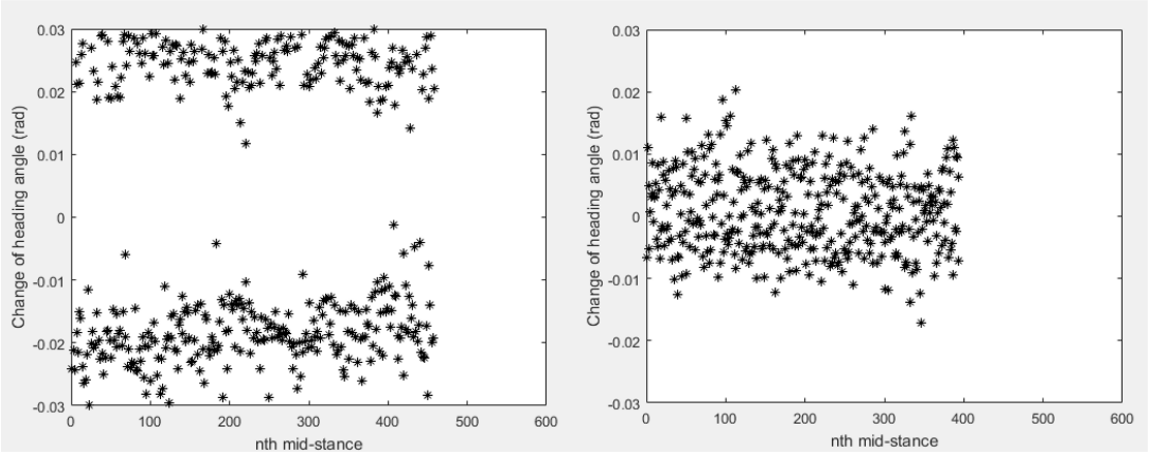

Figure 36: Rapid head angle changing versus slight heading angle change

Again, more advanced machine learning technique need to be implemented to verify and quantify our observation.

Chapter 4: Ongoing work on a directional Sensory Augmentation device

4.1 Hardware and algorithm

In this chapter, we describe ongoing work on the development of a sensory augmentation device to keep people walk on the desired trajectories, as they do not have the vision to guide them. For the time being, the current model is just to guide people to walk in a straight line with a limited sideway deviation tolerance. The device consists of an Arduino microprocessor, a GPS system, and two vibration motors. Figure 37 shows the inside of the device.

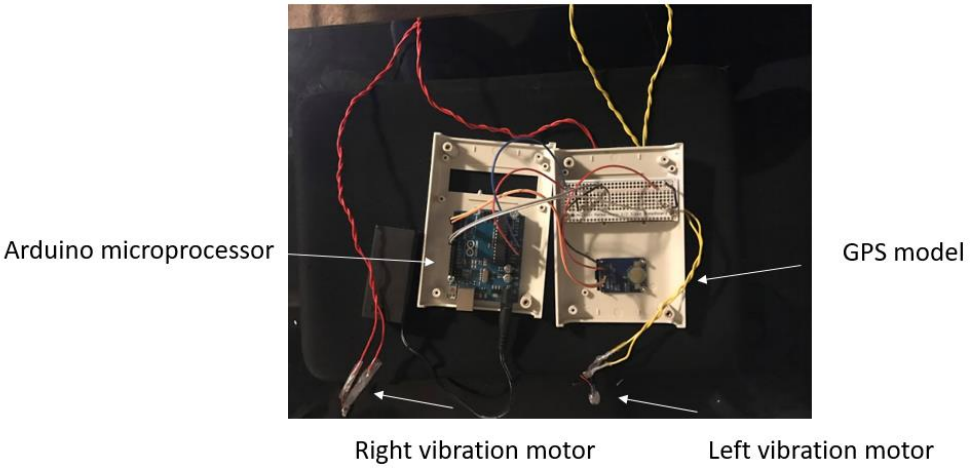

Figure 37: Sensory augmentation device

When in use, the user may hold the device in hand, or the device may be attached to the hip via a hip pouch. There will be one vibration motor on each side of the body (left and right), and one motor each may be placed in the pockets of clothes or attached to the body via straps, one on each side. If the GPS can get good data from the satellites, the device will send a vibrational

signal to the user so that user can start walking forward. During walking, if the left side vibrates, then the user is instructed to veer right and similarly, shift to the left if the right side vibrates. That is, the location of the vibration provides a signal to the user to move in the opposite direction – so as to avoid the vibration. Signals to the vibrational motors are updated at lower than 1 Hz so that the user has enough time to respond to the signal without getting too much unnecessary guidance.

The key course-correction algorithm is shown in Figure 38. The device receives GPS data every second and processes the data to obtain the local coordinate. After the device is activated, to obtain the "target straight line", we fit the first N data points with a straight line constrained to pass origin and define this line as the target trajectory, $y = kx$ where $k = \frac{\mu(x_i y_i)}{\mu(x_i^2)}$ [11]. We then generate two lines parallel to the target straight line and form a 2-meter tolerance band centered on side of the target straight line.

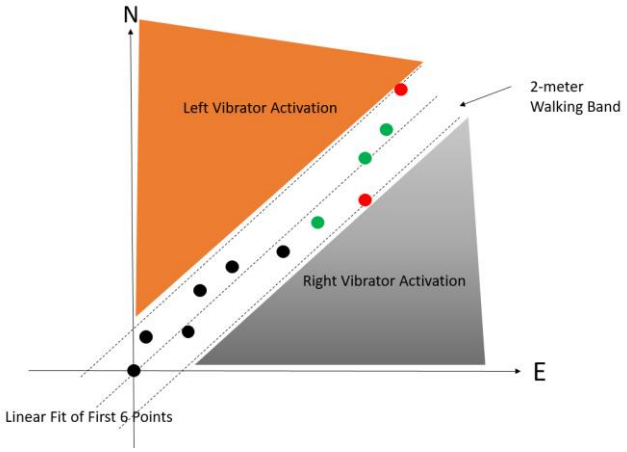

Figure 38: Device algorithm description

After the walking band is formed, the device will receive GPS data every 3 seconds, convert it to local coordinates, and judge if the current point is in or out of the walking band. If the current position is outside the target walking band, it will decide which side the data point shift to by the following mathematical principle by setting$b = 0$.

Let us assume the walking line is $y = kx + b$. Then, the corresponding 2-meter walking band boundaries are $y = kx + b + \frac{1}{\cos(atan(k))}$ and$y = kx + b - \frac{1}{\cos(atan(k))}$.

Alternatively, as shown in Figure 39, we can represent the straight target line in the following vector form: $u = u_0 + p \cdot s,\ u$ is the point on the line, u_0 is some initial point, and p is the desired unit vector walking direction obtained in the previous paragraph , and s > 0 is some scalar (s=0 at the initial point). We denote q as the unit vector perpendicular to p, obtained by rotating p anti-clockwise by 90 degrees:$q = e_z \times p$ **,** where e_z is the unit vector normal to the plane pointing towards the sky. Given the current location a_i converted from GPS data, with coordinate $\left(a_x, a_y\right)_i$ in the plane, we can determine the distance of the current point to the target straight line using the following formula: $D = |\overrightarrow{a_i u_0} \cdot q|$. If D > 1 m, the person is outside the target 2 m walking band. Further, we can determine whether the person is to the left or to the right of the walking direction using the following inequalities: left of the walking target if $\overrightarrow{a_i u_0} \cdot q > 0$ (leading to a left side vibration) and right of the walking band if $\overrightarrow{a_i u_0} \cdot q < 0$ (leading to a right side vibration).

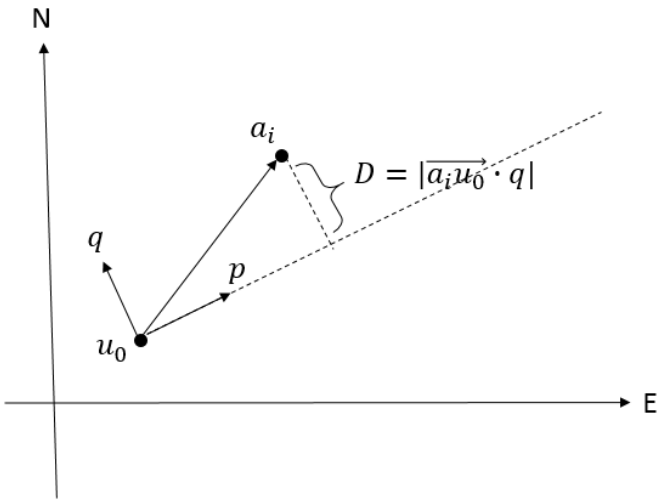

Figure 39: Algorithm used to determine the current position relative to the defined walking band

4.2 Current Status of device development

The above algorithm has been implemented in the device, and all the hardware are installed.

4.3 Future work

In the future, the device will be tested by blindfolded subjects and walking trajectories with the device is activated will be compared with their blindfolded walking trajectories without this device.

Besides, the algorithm described above can be modified to applicable to send the user from any current location to a target location as long as the subject not walking against the direction of the target location. In the original straight-line definition, we set the constraint that the line has to pass origin (the initial point); however, this constraint can be any point in R^2. For

example, as shown in Figure 40, assume user is walking with some initial data location $L_1, L_2, L_3, L_4\ and\ L_5$ and walking towards target location $T(T_x, T_y)$. We can generate straight line as $y = kx + b$ where:

$$k = \frac{covar(x, y) + (\mu(x_i) - T_x)(\mu(y_i) - T_y)}{var(x) + (\mu(x_i) - T_x)^2}$$

$$b = T_y - k \cdot T_x \text{ [11]}$$

Walking band equations are similar as above.

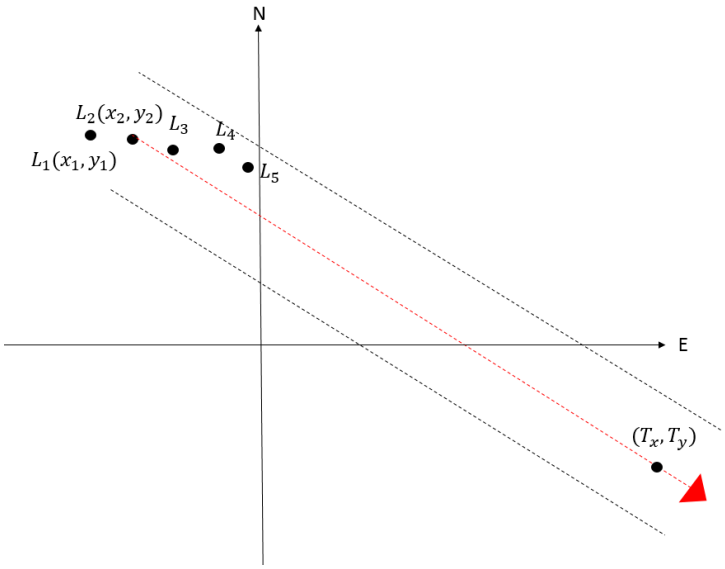

Figure 40: Target line towards target location

As shown in Figure 41, we can also modify the algorithm to track target polynomial trajectories, which can be defined by adding one or more constraints points (c_i) depending on the degree of generated polynomial. Walking on a curve can guide subject walking around obstacles and

allowing us to achieve more complex and useful autonomous walking behavior. Algorithm development for this situation will be part of future work.

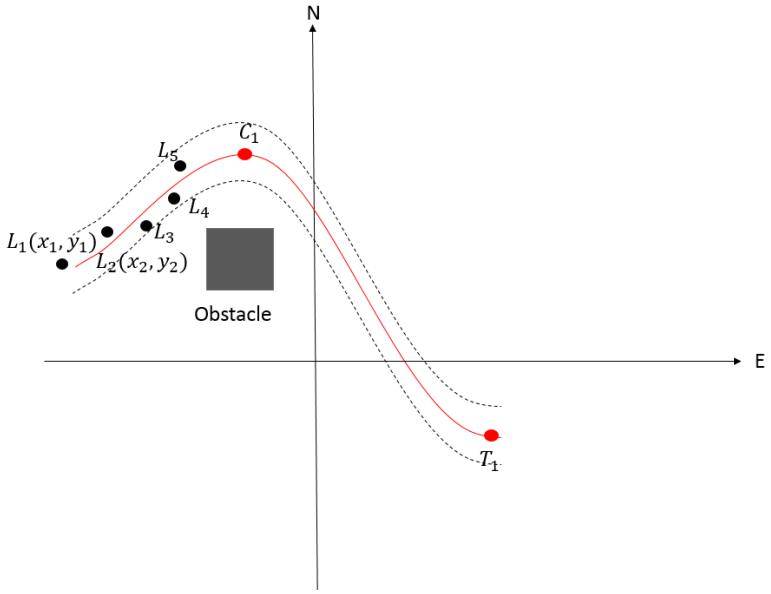

Figure 41: A hypothetical algorithm for autonomous walking

Chapter 5: Conclusion and Future work

In this research, blindfolded walking was furtherly studied toward determining what factors uniformly affect the outcome of blindfolded walking for general subjects, especially the veering behavior. We found that asymmetric knee stiffness or an asymmetric leg swing ratio can systematically influence the veering direction of the blindfolded walking, but an asymmetric ankle weight did not have an observable systematic effect. In the future, more asymmetric factors can be introduced into the experimental part so that "functional asymmetry" hypothesis mentioned by souman et al.[1] can be explored in more detail. The experimental part of this research can be improved by conducing more trials and get more subjects of different ages and physique involved. Also, more non-constraint blindfolded walking trial can be conducted to compare with the constrained walking trials so that the effect of asymmetric factors can be more clearly demonstrated.

We built a simple probabilistic model based on normal walking variability to simulate blindfolded walking. This model predicts veering of walking trajectory to one side or another depending on small asymmetries in the model. Future research could do experiments to verify such predictions or derive such models from blindfolded walking data rather than normal (non-blindfolded) walking data. The simulation part can be improved by making the model more realistic other than a three-point model. For example, leg mass and knee stiffness can be introduced into the model so that the foot stepping contact force can be computed and added to the regression model. It also worth mentioning that since our data set is based on normal walking with vision, many other factors contributing to the complexity of the blindfolded

walking was overlooked and the simulated trajectories were more idealized than the actual blindfolded walking trial. Thus, we would speculate that the obtained predictions may only be qualitative and not quantitative. We note that the model is purely data-based and does not use physics, but perhaps future models could incorporate physics-based dynamics modeling into the predictive model.

Finally, we presented early stage ongoing work for designing a mechatronic device providing sensory augmentation: a simple straight-line walking controller is built. We propose that further work may allow us to implement algorithms to guide people walk around obstacles autonomously, and to guide subjects to walk along higher order polynomial curve. In addition, more control strategies can be introduced into the controller other than just position control. For example, velocity and heading angle of the user can be traced to predict a potential tendency of walking outside the band.

Bibliography

1. Souman, J. L., Frissen, I., Sreenivasa, M. N., & Ernst, M. O. (2009). Walking Straight into Circles. *Current Biology, 19*(18), 1538-1542.

2. Sijie Yu, Experiments and Mathematical Modeling of Blindfolded Walking, Honors thesis, the Ohio State University, 2015

3. Bestaven, E., Guillaud, E., & Cazalets, J. (2012). Is "Circling" Behavior in Humans Related to Postural Asymmetry? (M. O. Ernst, Ed.). *PLoS ONE, 7*(9), E43861.

4. Christopher S. Kallie et al, "Variability in stepping direction explains the veering behavior of blind walkers"

5. Cheung, A., Zhang, S., Stricker, C., and Srinivasan, M. (2007). Animal navigation: The difficulty of moving in a straight line. Biol. Cybern. 97,47–61.

6. KELVIN E. JONES et al ,Sources of Signal-Dependent Noise During Isometric Force Production ,2002

7. Capaday C, "The special nature of human walking and its neural control." Trends Neurosci. 2002 Jul;25(7):370-6.

8. B. Hofmann-Wellenhof; H. Lichtenegger; J. Collins. GPS - theory and practice. Section 10.2.1. p. 282. ISBN 3-211-82839-7.

9. Y. Wang, M.Srinivasan "Stepping in the direction of the fall: the next foot placement can be predicted from current upper body state in steady-state walking".2014

10. Snijders CJ et al, Het Gaan, (https://eduweb.hhs.nl/~bergwandelen/onderzoek.htm), 1995.

11. Wikipedia, simple linear regression, https://en.wikipedia.org/wiki/Simple_linear_regression